FABRICATION TECHNOLOGY OF MM–Co PERMANENT MAGNETS

By

NAGESWARA RAO BONDA

DEPARTMENT OF METALLURGICAL ENGINEERING

INDIAN INSTITUTE OF TECHNOLOGY, KANPUR

JANUARY, 1981

FABRICATION TECHNOLOGY OF MM–Co PERMANENT MAGNETS

A Thesis Submitted
in Partial Fulfilment of the Requirements
for the Degree of
MASTER OF TECHNOLOGY

By

NAGESWARA RAO BONDA

to the
DEPARTMENT OF METALLURGICAL ENGINEERING
INDIAN INSTITUTE OF TECHNOLOGY, KANPUR

JANUARY, 1981

ME-1981-M-BON-FAB

CERTIFICATE

Certified that this work on "FABRICATION TECHNOLO OF MM-Co PERMANENT MAGNETS" by Nageswara Rao Bonda has been carried out under my supervision and that this has not been submitted elsewhere for a degree.

(E.C. SUBBARAO)
Professor
Department of Metallurgical Engineeri
Indian Institute of Technology
Kanpur

ACKNOWLEDGEMENTS

It was a great pleasure working under the guidance of Professor E.C. Subbarao. I am indebted to him for his excelle guidance and constant advice which made this work very inter- esting. I esteem very much the invaluable experience I gained under his supervision.

The most cordial and generous help of Prof. K.P. Gupta and Dr. A.K. Majumdar rendered to me in the form of advice and materials for experimental work, helped make the work especial pleasant.

I am greatly indebted to Dr. K.V.G.K. Gokhale for allowing me to work on Fisher Sub-Sieve Analyser for making particle size measurements.

I am very much thankful to Mrs. T.A. Padmavathi Shanka for her constant help throughout the work for analyzing my samples.

I am thankful to all the members of the project, Messers E.M.T. Velu, J. Subramanyam, S. Pandian, S. Laha and U. Ramakrishna, who took active participation in the discussi of the results of the work and put forward fruitful suggestio

I am thankful to Mr. Rajani and Mr. Yadav of Central Workshop, Mr. S.S. Sehgal, Mr. V.P. Srivastava and Mr. V.P. G who helped me at various stages of my work.

My thanks are due to Mr. Bajpai and Mr. D.B. Srivastava who prepared the tracings for this work. I am thankful to Mr. U.S. Mishra and Mr. R.N. Srivastava for the interest they have taken in typing the manuscript in an elegant form.

I am grateful to my friends Messers K. Ramesh Chowdary, V.V. Bhaskar, M.V.S. Bose, T. Hemadri and Jagan for their help at the final stages of this work.

My thanks are also due to Mr. Vishwanath Singh for his excellent cyclostyling work.

This work was carried out in a project sponsored by the Department of Electronics (Project No. DOE/ECS/MT/75-80) and the financial support provided by them is gratefully acknowledged.

- NAGESWARA RAO BONDA

TABLE OF CONTENTS

TABLE OF CONTENTS

LIST OF TABLES

LIST OF FIGURES

ABSTRACT

In the fabrication of MM-Co liquid phase sintered permanent magnets various process parameters play an important role in determining their magnetic properties.

In the present study, the dependence of $_iH_c$ of base material on milling time, average particle size and size distribution of powders prepared by ball milling, rod milling and EM pulveriser was studied and found that rod milling gives better $_iH_c$ values due to narrower particle size distribution. Chemical analysis of milled powders showed that there is deviation in the chemical composition from its original composition. Investigation of field pressing using a steady field and a pulse magnetise field showed that the field pressing process is not very efficient. Sintered and annealed magnets gave low $_iH_c$ values and this may be due to improper annealing treatment and partial oxidation.

INTRODUCTION

The usefulness of a material for permanent magnets is primarily determined by its demagnetisation curve and depends in particular on the maximum value which the product (BH) attains as this curve is traversed. Stages in the race to reach ever higher values of $(BH)_{max}$ were the development of tungsten steel in 1900 (with a $(BH)_{max}$ of 0.34×10^6 G Oe), cobalt steel in 1917 (0.9×10^6), 'Triconal' II in 1936 (1.8×10^6), 'Triconal' G in 1937 (15.0×10^6), 'Triconal' GG in 1949 (8.3×10^6), Platinum-cobalt (gradually raised since 1936 to 10.5×10^6 in 1966) and 'Triconal' XX in 1956 (11.0×10^6). Later it was found possible to increase the $(BH)_{max}$ value of the last-mentioned material to 13.4×10^6 G Oe[1].

The search for still better magnetic materials is guided by the consideration that such materials should combine high values of saturation magnetisation with high H_c. This combination can be found in intermetallic compounds of cobalt and rare-earths. The excellent properties of permanent magnets based on the compounds $R Co_5$, where R is a rare earth metal, were first predicted by Strnat[2]. A particular material that has attracted attention in recent time is Sm-Co compound $Sm Co_5$.

I.1 Origin of magnetism in R-Co alloys:

The atoms of most of RE metals (general symbol R) have a magnetic moment of their own because of the unpaired electrons in the completely filled 4f shell, and this moment is generally a multiple of that of a cobalt atom. An intermetallic compound like R Co_5 may therefore be expected to have a high magnetic saturation if there is 'ferromagnetic coupling' between the magnetic moments of the R and the Co atoms i.e. if these align themselves parallel to one another. In the lighter rare-earth compounds this does in fact happen. The magnetic moment of the lighter rare-earth (J = L-S) adds to that of cobalt and hence leads to a higher magnetisation value.

I.2 Crystal structure of R Co_5 compounds:

R Co_5 compounds have a Ca Cu_5 type of crystal structure. This structure shown in Figure I.1 (after Mc Curie et al[3]) contains one formula unit per cell. The R atom is at 000; two Co atoms at 1/3 2/3 0; 2/3 1/3 0; and three Co atoms at $\frac{1}{2}$ 0 $\frac{1}{2}$; 0 $\frac{1}{2}$ $\frac{1}{2}$; and $\frac{1}{2}$ $\frac{1}{2}$ $\frac{1}{2}$[4].

This structure consists of two different layers of atoms. One type of layer consists of a hexagonal arrangement of Co atoms. The other layer is composed of two kinds of atoms in the proportion of one R atom to two Co atoms.

The hexagonal crystal structure coupled with the high magnetocrystalline anisotropy is the fundamental factor which

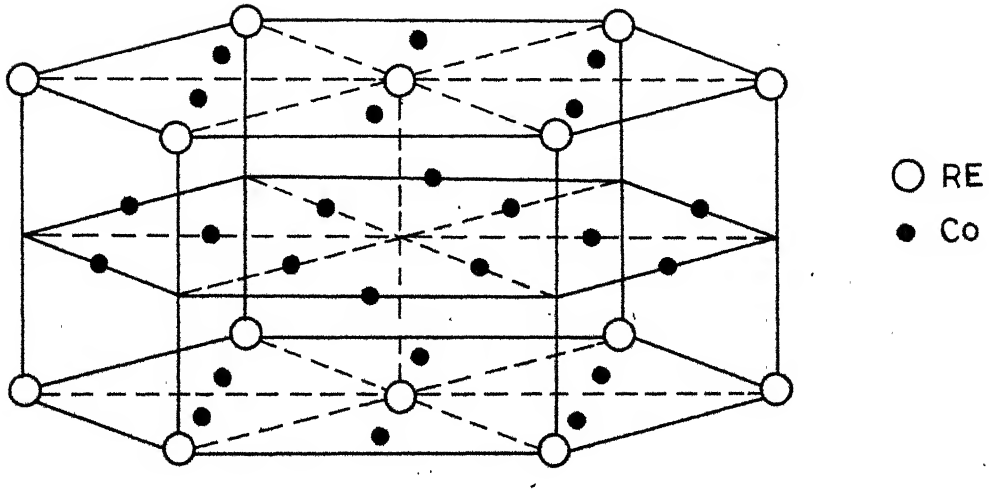

FIG. I.1 Crystal structure of $RECo_5$ compounds. (Ref. 3)

accounts for the high coercive force of the R Co_5 compounds. The preferred direction of the magnetic moments of R Co_5 is generally c-axis. The anisotropy field H_A i.e. the field strength needed to align the magnetic moments perpendicular to their preferred direction is as much as 290 K Oe in the case of Sm Co_5. H_A is given by

$$H_A = 2K/M_s \qquad (1)$$

where K = anisotropy constant

M_s = saturation magnetisation

values of M_s, K and H_A for some of the R Co_5 compounds are listed in Table I.1

Table I.1 : $4\pi M_s$, K and H_A for some R Co_5 compounds[5]

Compound	$4\pi M_s$ (KG)	K 10^7 ergs.cm^3	H_A K Oe
Y Co_5	10.6	5.5	130
La Co_5	9.1	6.3	175
Ce Co_5	7.7	5.2	170
Pr Co_5	12.0	6.9	145
Sm Co_5	10.7	11.2	290
MM Co_5	8.9	6.4	195

Provided the grains of the material are small enough, so that they contain no mobile domain walls whose displacements permit relatively easy demagnetisation, the H_c could in theory reach the exceptionally high values mentioned above.

The combination of properties should theoretically enable permanent magnets with $SmCo_5$ as the base material to reach a $(BH)_{max}$ of more than 23 MG Oe which is much higher than is obtainable with other compounds from RCo_5 series.

I.3. Techniques for preparation of rare earth-cobalt permanent magnets

Previously making magnets from rare earth cobalt alloys have centered around two processes. The first, and oldest, involves grinding a RCo_5 alloy into micron-size particles, aligning the powder in a magnetic field, and pressing to a density of impregnating with a plastic or other non-magnetic material. The second process is sintering which also involves field alignment and pressing of fine powder but ends with a high temperature sintering treatment to densify the magnet to over 90% of full density. Sintering process was studied extensively as it would result in high density and tend to correct the misorientation of unaligned particles. Alignment and density are very important factors as they influence magnetic properties.

Afterwards, liquid-phase sintering was applied to the preparation of these magnets, which is being most extensively used due to its advantages over solid-phase sintering process.

I.3.1. Techniques without sintering

In their first experiments with $SmCo_5$ compound, Buschow, Luiten, Naustepad and Westendorp[6] were able to reach

values of 8.1 MG Oe. The starting material for the magnets was obtained by melting together Sm and Co in a protective gas atmosphere, powdering the product of the melt and then subjecting the Sm Co_5 powder to prolonged grinding. After the grinding, the powder was mixed with a binder and then grain-oriented in a magnetic field and compacted. One of the purpos of the binder is to ensure that the orientation of the Sm Co_5 particles and hence their magnetic moment remains fixed.

The fact that the $(BH)_{max}$ obtained in this was still far below the theoretically attainable values was partly attributed to the high porosity of the compacted body; the relative bulk density was only 70 percent.

By using a new pressing technique, Buschow et al[7] produced Sm Co_5 compacts of 95 percent relative density with $(BH)_{max}$ of 20 MG Oe. This technique is a complex pressing process including isostatic pressure upto 20 K bar with additional uniaxial deformation involving a total pressure of around 30 K bar. Generally no binder is used during cold pressing since the use of binders such as PVA did not lead to better results.

A new modification of the preparation method for Sm Co_5 magnet was studied by Umebayashi and Fuzimura[8]. This method involves compacting the field-oriented pellet of the alloy powder through a solid state pressure transmitting medium in a conventional axial pressing apparatus. The magnets with the packing fraction of 87% and $(BH)_{max}$ of 15 MG Oe were obtained by this method.

It was found that an essential improvement of the particle alignment was achieved in the field-orientation process when the powder was pressed in the perpendicular, rath than parallel, direction to the magnetic field[8].

I.3.2 Solid-phase sintered magnets:

Sintering of aligned fine particle Sm Co_5 powder was attempted by Das[9] to achieve magnets with high density, high coercivity and high energy product. His results are remarkable in that he reports that sintering for 1 hour at 1000°C in an inert atmosphere yielded a magnet with a density of 8.5 g/cc (about 99 percent dense). The magnetic properties reported (B_r = 8-9 KG, $_BH_c$ = 8-9 k Oe and $(BH)_{max}$ = 16-20 MG Oe) were comparable to those reported by Buschow[7] for the mechanical compaction methods.

Initial attempts to sinter the stoichiometric Sm Co_5 alloy failed because of loss of coercivity during sintering[10]. Though good densities were obtained at high temperatures, there was serious loss of H_c, due to the grain growth accompanying densification. The $_iH_c$ dropped from 12 k Oe to 2 k Oe for Sm Co_5 magnets. In addition there was a loss of $_iH_c$ during long time exposure to air at slightly elevated temperatures.

It was found that hyperstoichiometric compositions could be sintered to a high density without loss of coercivity. According to Benz and Martin[11] and Cech[10], the excess Sm than allowed by stoichiometry is beneficial for the following reason

The rare earths tend to oxidise more easily than Co and, therefore the extra Sm ensures availability of adequate amou for the formation of Sm Co_5. Therefore Sm-rich Sm Co_5 magne were prepared by sintering.

In the case of solid phase sintered MM Co_5 permanent magnets alloys (where MM is Ce-rich misch-metal) Nagel and Menth[12] have extensively studied the role of MM in MM Co_5 and (Sm, MM) Co_5 magnets. They have shown that in (Sm_xMM_{1-x}) Co_5 where $0 < x < 0.4$, the $_iH_c$ value increases (from 9 k Oe to 24 k Oe) whereas the increase in $(BH)_{max}$ is less pronounce (from 14.5 MG Oe to 18 MG Oe).

For lower Sm concentrations in (Sm, MM) Co_5 alloys, Ratnam and Wells[13] improved the hard magnetic properties. For Sm concentrations between 6-9 wt percent of the final composition, they prepared magnets with $(BH)_{max}$ in the range 14-15 MG Oe, depending on the method of preparation.

But still the problem of loss of $_iH_c$ when exposed to air at elevated temperatures existed in these solid phase sintered R Co_5 magnets.

The best properties were so far obtained for an alloy of Co, 25.5 wt% Sm, 8 wt% Cu, 15 wt% Fe, 1.5 wt% Zr by Ojima et al[26]. The energy product of this alloy is 30 MG Oe. This is achieved by a step tempering following the sintering treatment.

I.3.3 Liquid phase sintered magnets:

In view of the above problems Benz and Martin[14] outlined a novel approach i.e. liquid phase sintering of Sm-rich Sm Co_5. They found that

a) Liquid-phase sintering of Sm-Co is effective for preparation of high H_c, high energy product magnets.

b) Sintering to a closed-pore structure eliminates the loss of magnetic properties during longtime exposure to air at elevated temperatures normally observed for open-pore structures.

c) Energy products in excess of 20 MG Oe can be obtained for Sm Co_5 magnets.

Liquid-phase sintering consists of sintering of base material in presence of an additive having the composition richer in rare earths which melts at the sintering temperatures. After pulverising, base material and additive are mixed in such a proportion that the final composition in R rich R Co_5. Additional rare earth will take of oxidation during sintering. Prior to sintering the powders are field-pressed and hydrostatically pressed.

This is the most widely used technique now-a-days for R-Co magnet preparation and it has been studied over a variety of R-Co compositions.

I.3.3.1 Sm-Co magnets:

Benz and Martin[14] prepared Sm-Co magnets by liquid phase sintering in the following way:

A melt of essentially $SmCo_5$ was prepared by induction melting. This was crushed to coarse powder in a mortar and pestle. It was then further reduced to an average particle diameter of 6-8 μ by grinding in a fluid energy will using nitrogen as the working gas. A second of Co + 60 wt% Sm was processed in a similar manner. This composition was selected as one of a series of compositions that would have a liquid-phase component at the sintering temperature of 1100°C. Chemical analysis indicated 66.7 wt% Co for the first and 40% Co for the second. The two powders were blended by tumbling to an average composition of 62.6% Co. This composition is in the range which produces maximum densification during sintering as discussed by Cech (unpublished). Portions of this powder were placed in rubber tubes $\frac{3}{8}$" (0.98 cm) in diameter and $1\frac{3}{4}$" (4.45 cm) long and packed to a density of 3.5 g/cc. These tubes of powder were placed in an axial magnetic field of 60-100 k Oe in order to allign the powders. After aligning, the rubber tubes were evacuated and then the samples were subsequently hydrostatically pressed to 2×10^5 psi. The pressed density was approximately 6.9 g/cc. The resultant bars were then ground to cylinders 1/4" (0.64 cm) in diameter by $1\frac{1}{4}$" (3.18 cm) long. Subsequent sintering for 1/2 hr at 1100°C in high-purity argon increased the density to approximately 7.7 g/cc. Metallographic examination of the sintered bars showed approximately 10% void

volume. These voids were of the non-interconnecting type.

Magnetic properties of Sm-Co magnets are difficult to measure because of the need for extremely high fields for saturation and demagnetisation. They have used a 100 k Oe niobium-tin superconducting solenoid for their measurement.

Table I.2 Summary of magnetic properties of Sm-Co magnets[14]

Sample No.	Density (g/cm^3)	Saturation magnetisation at k Oe (k G)	B_r (k G)	$_BH_c$ k Oe	$_MH_c$ k Oe	$(BH)_{max}$ MG Oe
A	7.56	9.47	8.05	-7.7	-15.7	15.7
B	7.56	9.41	7.98	-7.8	-14.8	15.7
C	7.58	9.50	8.06	-7.7	-16.2	15.7
D	7.62	9.42	8.06	-7.7	-16.4	15.7
D*	7.62	9.37	7.98	-7.4	-16.4	15.4

* after 1145 hours at 150°C in air

Data gathered is listed in Table I.2 for several sintered Sm-Co magnets. The demagnetisation curves for one sample before and after exposure at 150°C for 1145 hours are shown in Figure I.2. The slight difference in properties before and after 150°C aging is not considered significant, being less than the estimated measurement error at the time of this study. By improvements in alignment and packing, subsequent samples with $(BH)_{max}$ in excess of 20 MG Oe have been reported by these authors.

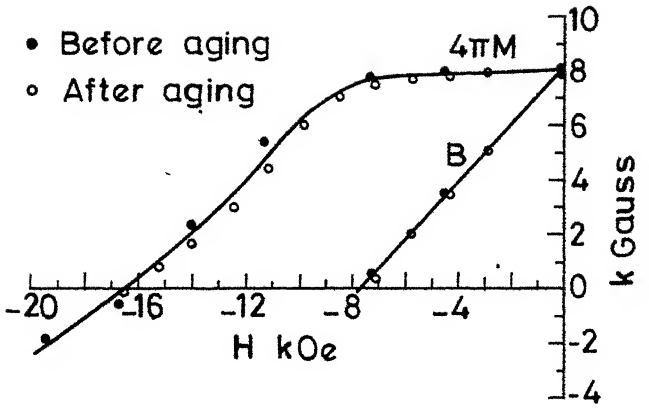

Fig.I.2 Magnetization and induction curves for sample D.(Ref.14)

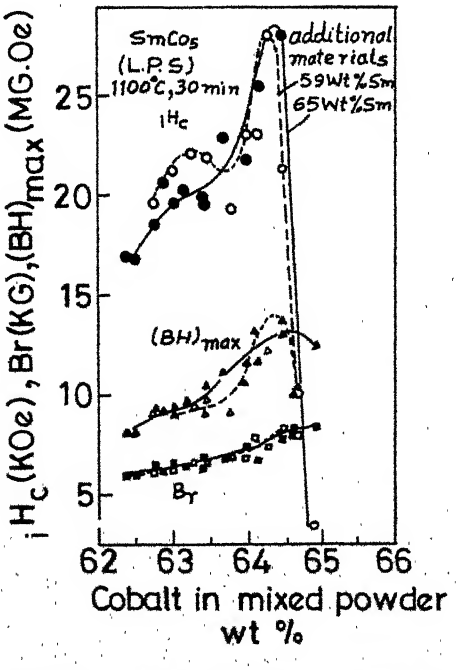

Fig.I.3 Composition dependence on the magnetic properties of a series of Sm-Co permanent magnets made by liquid phase sintering. (Ref.15)

Shibata and Katayama[15] studied the liquid phase sintering of Sm-Co by using various additives and found the optimum Co content to get optimum results. Figure I.3 shows the composition dependence of magnetic properties for a Sm-Co series. These samples were obtained by using Sm Co_5 as the base material and using 59 wt% Sm-Co and 65 wt% Sm-Co as additives respectively. These samples were prepared by sintering at 1100°C for 30 min. Optimum properties were obtained for a mixed powder with Co wt% of 64.3. As a result the magnetic properties for Sm-Co alloy sintered for 30 min at 1100°C were determined solely by the amount of Co content and they did not depend on the kinds of additive materials atleast in the range of Co wt% between 56% and 65%. Single phase Ca Cu_5 type after sintering was observed.

Another result of their best results was obtained in the Sm-Co alloy, where B_r = 8.6 k G, H_c = 8.6 k Oe and $(BH)_{max}$ = 18.0 MG Oe. It was obtained for a sample with 64 wt% Co and with a particle size of about 10 μm.

Johnson and Fellows[16] determined the effect of composition, sintering temperature and compaction pressure on the properties of Sm Co_5 magnets. Sm Co_5 powders containing 63 and 66 wt% Co were blended with Sm-Co sintering additives containing 70 or 73 wt% Sm to give powder mixtures with different composition. Aligned compacts were uniaxially pre-pressed to 2 k bar and isostatistically pressed at 3 k bar and the effect of sintering for 1 hour at various temperatures is determined. Higher sintering temperature generally led to better densification,

this being accompanied by a tendency for $_{J}H_{c}$ to decrease. Compacts having Co content of 59 wt% could be sintered at temperature upto atleast 1160°C with serious loss of $_{J}H_{c}$ and with satisfactory densification while those from mixtures having 63 wt% Co content had $_{J}H_{c}$ values which are lower at all the sintering temperatures used and decreased sharply at temperatures about 1120°C. This comparatively low sintering temperature gave only limited densification and poor levels of B_r and $(BH)_{max}$. It was concluded that the high sintering temperature necessary to give adequate densification after compaction at 3 k bar could only be used if the total Sm content was considerably in excess of the stoichiometric composition of $Sm\ Co_5$. Finally, another mixture was prepared with a Co content intermediate between the previous levels; a sample compacted as previously described and sintered at 1140°C has much superior properties (B_r = 8.1 k G, H_c = 8.05 k Oe, $(BH)_{max}$ = 16.4 MG Oe).

In another study by the same authors[16], two mixtures having almost the same Co content were used to produce aligned compacts, uniaxially field pressed to 2 k bar and isostatically pressed in rubber to between 3 and 7 k bar. Compact properties after sintering at 1140°C for 1 hr showed that increasing isostatic pressure from 3 to 6 k bar gave some improvement in sintered density with subsequent improvement in $(BH)_{max}$ upto 18.0 MG Oe. A further increase in $(BH)_{max}$ upto 18.4 MG Oe, observed on increasing to pressure to 7 k bar was not caused by an increase in density but was probably due to the slightly

higher Co content (from 60.1 to 60.9) and specific saturation of the powder mixture (from 78 to 80 emu/g). It was also observed that there was clearly no real difference between pressing isostatically in rubber to 4 k bar and conventional isostatic pressing in which the pressing medium was a fluid, after similar sintering treatments.

Fonel et al[24] reported an energy product of 24 MG Oe for Sm-Co alloy. A $SmCo_5$ base metal powder and a 60 wt% Sm + 40 wt% Co additive powder were blended to a nominal composition of 36 wt% Sm. By optimising parameters of fabrication, nearly complete alignment of the magnetic properties was achieved with a relative density which is 95% of the theoretical maximum. Sintering was done at 1135°C for 1 hr in an argon atmosphere. The sample was given a post sintering treatment of 20 min at 1100°C, slow cooled to 850°C, held for 1 hr at that temperature, and cooled rapidly to room temperature.

Jones et al[27] prepared Sm-Co magnets by mixing two powders, having the composition of 34 wt% Sm and 42 wt% Sm to a nominal composition of 39 wt% Sm. Sintering was done at 1100-1140°C for 1 hr in hydrogen atmosphere. The use of hydrogen atmosphere led to substantially improved magnetic properties. The major improvement was in the magnetic induction. Specimens sintered in hydrogen atmosphere attained higher densities ($P > 98\%$) than those sintered at temperature upto 40°C higher in argon. The degree of improvement in magnetic properties was greater than it could be accounted for by the increased density. They obtained $(BH)_{max}$ = 21.6 MG Oe,

B_r = 9.56 k G and H_c = 9.13 k Oe at the sintering temperature of 1120°C.

Magnets sintered in hydrogen showed a pronounced difference in shrinkage behaviour compared to those sintered in argon. The ratio of the shrinkage in the preferred magnetic direction to that in the cross-section was greatly reduced in hydrogen.

I.3.3.2 Pr-Co Magnets:

Tsui and Strnat[17] applied liquid-phase sintering successfully to pure Pr Co_5, using as additives either an alloy of 60 wt% Sm and 40 wt% Co or one of 70 wt% Pr and 30 wt% Co.

The nearly single-phase Pr Co_5 and the two additive alloys were individually attritor milled under toluene. The powders were then vacuum dried, intimately blended in the desired ratios, and then pressed into prismatic brick samples in a die with a uniaxial pressure of 1.25×10^5 psi while a 36 k Oe field was applied perpendicular to the force direction. The bricks were sintered in quartz tubes under vacuum for 30 min at different temperatures ranging from 1000 to 1160°C. The grinding time, the weight ratio of Pr Co_5 and the additive, and the sintering temperature were systematically varied to find optimum conditions. Details about the experiments aimed at finding the optimum sintering conditions for Sm-free binary Pr-Co magnetic alloys were reported.[18]

The magnet of highest energy product that was produced using Pr-Co as the sintering aid had the following properties. B_r = 8.53 k G, $_MH_c$ = 5.54 k Oe, $_BH_c$ = 4.98 k Oe, $(BH)_{max}$ = 16.6 MG Oe, a residual to peak magnetization ratio M_r/M_p = 0.97 and a density d = 7.93 g/cm^3. However, the highest $_MH_c$ obtained in another sample was 9.47 k Oe, a four-fold increase over the value before sintering. This was combined with B_r = 5.38 k G and $(BH)_{max}$ = 6.8 MG Oe.

Pr Co_5 magnets made with the Sm-Co additive as a sintering aid has generally higher coercive forces, greater densities, and consequently higher energy products. Again, one can trade off coercivity for remanence to some extent. The best properties obtained in this series were B_r = 9.21 k G, $_MH_c$ = 12.67 k Oe, $_BH_c$ = 7.14 k Oe, $(BH)_{max}$ = 21.1 MG Oe, M_r/M_p = 0.98 and d = 8.16 g/cm^3. The highest coercivity was $_MH_c$ = 14 k Oe much higher than before sintering ($<$6.0 k Oe), combined with $(BH)_{max}$ = 9.8 MG Oe.

Demagnetisation curves for representative samples of each of the two groups are shown in Figure I.4. Sintering process parameters are listed in Table I.3

Table I.3 Sintering process parameters

	Additive		Sintering	
Type	Quantity (wt%)	Total nominal rare earths (wt%)	Temp. (°C)	Time min
Pr-Co	20	38.2	1120	30
Sm-Co	25	39.2	1140	30

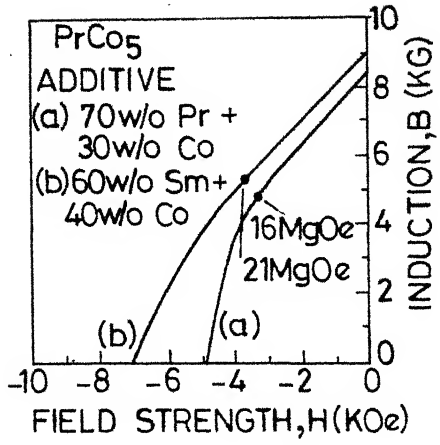

Fig.I.4 Demagnetization curves for sintered $PrCo_5$ magnets with two different sintering aids. w/o designates wt%. (Ref.17).

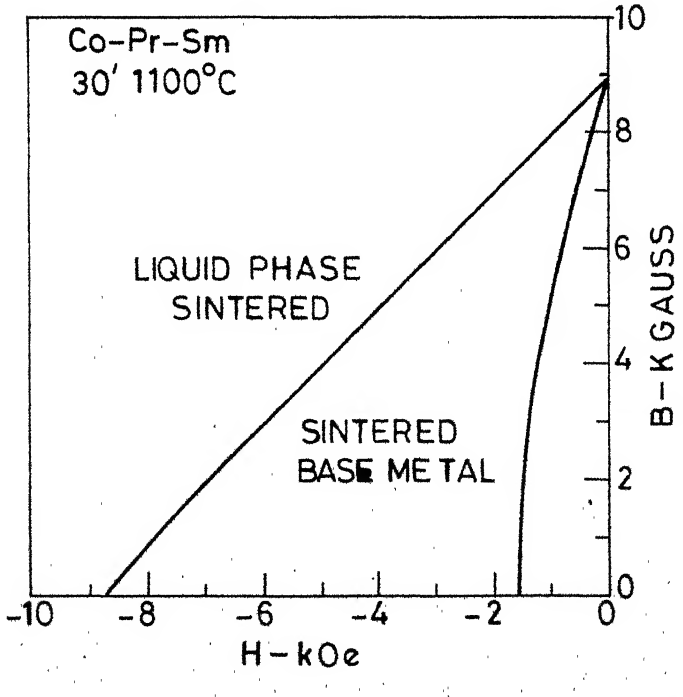

Fig.I.5 Comparison of B:H curves for a liquid phase sintered magnet and for a magnet made from the same base metal ($Co_5Pr_{0.5}Sm_{0.5}$) by normal solid state sintering.(Ref.19).

Composition dependence of magnetic properties of powder magnets prepared by liquid phase sintering process and if the non-sintered samples in the series of Sm-Pr-Co was studied by Shibata and Katayama[15]. The non-sintered specimens were aligned in a field of 16 k Oe and were fixed with epoxy resin. Coercive force, magnetic remanance and maximum energy product have their optimum values around $Sm_{0.5}\ Pr_{0.5}\ Co_5$. Sintered samples have these maximum values around $Sm_{0.3}\ Pr_{0.7}\ Co_5$. They obtained a megnet of near $Sm_{0.3}\ Pr_{0.7}\ Co_5$ alloy with $(BH)_{max}$ = 20 MG Oe, $_iH_c$ = 10.6 k Oe and B_r = 9.7 k G.

Martin and Benz[19] reported magnetic properties of R-Co magnet using $R\ Co_5$ as base metal where R is one of the rare earth metals or a combination of rare earth metals. The additive used in this study was a Sm +40 wt% Co alloy. Table I.4 gives the properties of some of these magnets. Figure I.5 shows the comparison of demagnetisation curve for liquid phase-sintered magnet and for a magnet made from the same base metal ($Sm_{0.5}\ Pr_{0.5}\ Co_{5.0}$) by normal solid phase sintering.

Table I.4 Magnetic properties of some Rare-earth cobalt alloys.

mple.	Base Metal	Blend (% Co)	Sintering (Hr)	°C	B_r (k G)	$_BH_c$ (k Oe)	$(BH)_{max}$ MG Oe	Packing (p)	Alignment A
1	$Sm_{0.5}Pr_{0.5}Co_5$	63	0.5	1100	9.50	8.30	22.2	0.97	0.95
2	$Pr\ Co_5$	62	1.0	1110	9.36	5.20	14.0	0.95	0.90
3	$Sm_{0.5}Pr_{0.5}Co_{5.0}$	*	0.5	1100	8.90	1.55	5.4	0.92	0.81
4	$Sm_{0.5}La_{0.5}Co_{5.0}$	64.5	0.5	1105	7.27	7.10	13.2	0.94	0.90
5.	$Sm_{0.5}Ce_{0.5}Co_{5.0}$	62	0.5	1100	7.66	3.80	13.5	0.97	0.95
6	$Sm_{0.5}M_{0.5}Co_{5.0}$	63	1.0	1070	7.88	6.70	15.2	0.95	0.96

By optimization of composition and sintering heat treatment, the following properties of a Sm-Pr-Co permanent magnet were achieved by Charles et al[20]:

$$J_r = 10.26 \text{ k G}$$

$$_BH_c = 10.13 \text{ k Oe}$$

$$(BH)_{max} = 26.0 \text{ MG Oe}$$

It was also shown that the magnetic properties of such magnets are highly sensitive to variations in composition and sintering temperature. Base metal used was $Sm_{0.24}\ Pr_{0.76}\ Co_5$ and additive powder was Sm + 40 wt% Co. The above properties were obtained for a final nominal composition of 15.8 wt% Sm, 21.3 wt% Pr and 62.9 wt% Co. Sintering was done at 1120°C for one hour.

By using 63-64% Co (in wt), 16.5% Pr and 19.5-20.5 Sm as base material and $Fe_2\ Sn$ as additive (0.5% $Fe_2\ Sn$ was added during ball milling) Hou-ting[28] produced magnets having $(BH)_{max}$ = 25.5 MG Oe, B_r = 10.45 k G and $_BH_c$ = 9.75 k Oe.

The sintering temperature is 1090-1100°C for a period of 30-60 minutes. Since Pr-Sm-Co permanent magnets with additive Fe_2 Sn do have relatively high H_c, the Fe_2 Sn alloy considered to be capable of both decreasing the sintering temperature and preventing the crystal grains from over-growing.

I.3.3.3 Sm-MM-Co magnets:

The substitution of misch metal for Sm in Sm-Co permanent magnet alloy is desirable because if the greater abundance of the misch metal. Misch metal is a Cerium-rich rare earth alloy of the following nominal composition: 50 wt% Ce, 27 wt% La, 16 wt% Nd, 5 wt% Pr , 2 wt% other rare earth metals. The studies of Benz and Martin[21] have shown that a substantial fraction of the Sm can be replaced by MM without any appreciable loss of magnetic properties.

In order to study the effect that cobalt content has on the magnetic properties, several compositions were prepared by blending a 66 wt% Co, 17 wt% MM, 17 wt% Sm alloy powder with a 40 wt% Co and 60 wt% Sm alloy powder. Blended powders were oriented in a magnetic field of 60 k Oe and then compacted to a relative density of 80% by application of hydrostatic pressure upto 200 k psi. Figure I.6 shows the variation of magnetic properties with Co content when sintered at 1000°C for 1/2 hour.

The intrinsic coercive force $_JH_c$ and $(BH)_{max}$ seemed to peak in the 63-66 wt% Co region. With the sintering treatment used, however the relative density achieved was less than 86%.

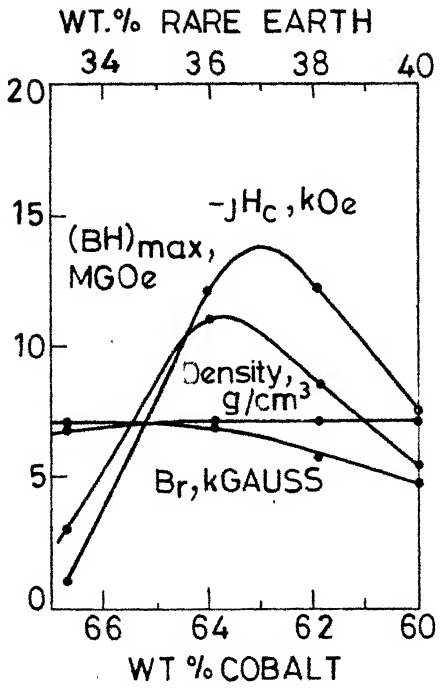

Fig.I.6 Magnetic properties of a series of cobalt-rare-earth alloys sintered for $\frac{1}{2}$ h at 1000°C. (Ref 21)

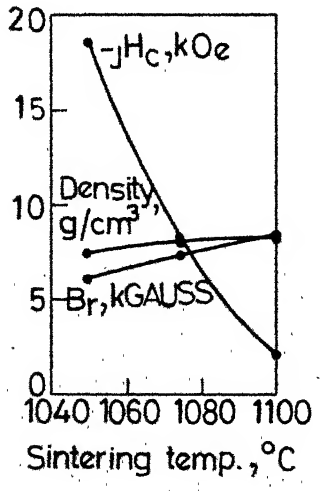

Fig.I.7 Magnetic properties of a 63.9 wt%-cobalt alloy as a function of sintering temperature. The samples were sintered for $\frac{1}{2}$ h. (Ref. 21)

In an effort to increase the density and hence the remanant flux density B_r and $(BH)_{max}$. the samples containing 63.9 wt% Co were sintered for 1/2 hour at 1050°C, 1075°C and 1100°C. As shown in Figure I.7, the density increased to 8.2 g/cm^3 (True density was taken as 8.4 g/cm^3), the B_r increased to 8.4 k G, but the $_JH_c$ dropped to -2.1 k Oe. This drop in coercivity was disappointing and meant that a high $(BH)_{max}$ could not be achieved by sintering to such a high density unless some post sintering treatment could be developed which would raise the coercivity. Figure I.8 shows the improvement of coercivity after various thermal treatments. The composition for sample H was 63.9 wt% Co. The curve H1 was taken after sintering for 1/2 hour at 1100°C, the curve H2 after a subsequent aging treatment at 1000°C for 19 hours; the curve H3 after an additional aging treatment of 900°C for 16 hours; and the curve H4 after an additional aging treatment at 800°C for 16 hours. The composition for sample I was taken 63.0 wt% Co. The curve I3 was taken after sintering for 1/2 hour at 1075°C and aging at 900°C for 16 hours.

The original composition study (Figure I.6) was then repeated with the use of the higher sintering temperature, 1 hr at 1075°C and aging by furnace cooling to 900°C or 950°C, and holding overnight at that temperature. The magnetic properties for these samples are plotted as a function of cobalt content in Figure I.9. As in Figure I.6, the $(BH)_{max}$ seemed to peak in the 63-64 wt% Co region. The values are much higher, however.

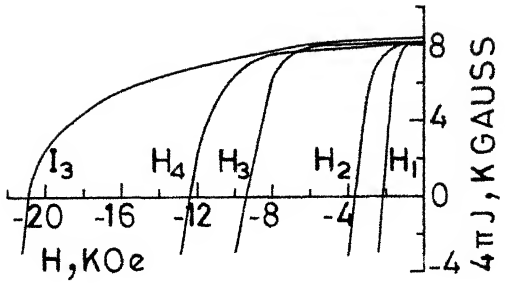

Fig.I.8 Magnetization curves after sintering and aging. (Ref. 21)

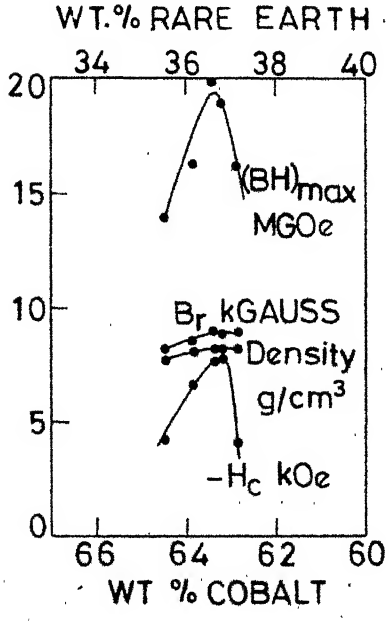

Fig.I.9 Magnetic properties of a series of cobalt-rare-earth alloys sintered for 1 h at 1075°C and aged for 15h at 900° or 950°C. (Ref. 21)

I.3.3.4 MM-Co magnets:

Because of its relative cheapness the use of MM rather than the pure rare earth metals would have considerable economic advantages. Mc Caig[22] reported the properties of MM Co_5 compacts by isostatic pressing without sintering and having $(BH)_{max}$ upto 3.1 MG Oe. A preliminary examination of the properties of liquid phase sintered R Co_5 magnets based entirely on MM has been carried out by Johnson and Fellows[16]. The results are shown in Table I.5. Two different additives were used.

Table I.5 Properties of R Co_5 magnets containing MM

Composition of sintering additive	Sintering Temp °C (Sintering time 1 hr)	Sintered density g/cm^3	Magnetic properties B_r k G	H_c k Oe	$(BH)_{max}$ MG Oe	$_JH_c$ k Oe
84.0 wt% MM	1030	7.4	5.00	2.70	4.2	3.40
(Co content	1080	8.1	5.90	1.38	4.4	1.50
of mixed	1120	7.9	5.10	0.91	2.8	0.94
powder = 57wt%)	1160	7.6	4.60	0.57	1.0	0.63
73.0 wt% Sm	1025	7.6	5.90	4.25	9.0	-
(Intended	1050	7.8	6.50	4.95	10.6	-
composition	1060	8.1	5.95	4.15	8.7	-
61 wt% Co,	1075	8.1	6.50	2.60	4.7	-
7.8 wt% Sm,						
31.2 wt% MM)						

Figure I.10 shows the demagnetisation curves of a Sm Co_5 magnet and a MM Co_5 prepared by liquid phase sintering using 73 wt% Sm + 27 wt% Co as additive and magnetised in a pulsed field of 100 k Oe. Samples in Table I.5 were magnetised in a pulsed field of 50 k Oe.

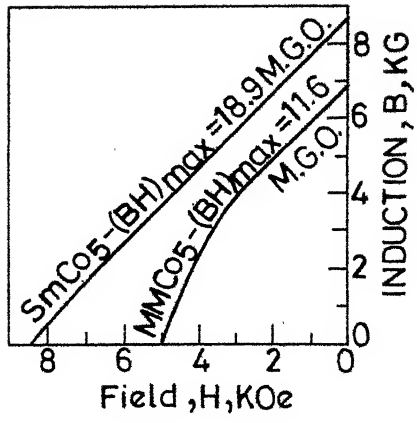

Fig.I.10 Demagnetization curves of a $SmCo_5$ magnet and a $MMCo_5$ magnet prepared by liquid-phase sintering and magnetized in a pulsed field of 100 KOe. (Ref.16).

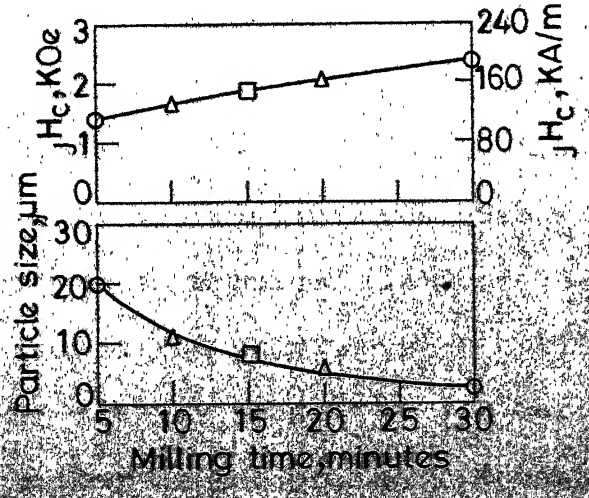

Fig.I.11 Variation of $_JH_c$ and particle size of $MMCo_5$ powders with milling time (Ref 23)

o Co 63.9 wt%
Δ Co 64.5 wt%
□ Co 63.9 wt%

According to Strnat, the $(BH)_{max}$ of MM Co_5 could, in theory, approach 20 MG Oe[23]. Several of the factors involved in the preparation of MM Co_5 permanent magnets have been studied by the same authors[23] with the aim of achieving a useful level of properties.

Two groups of castings, with the aimed compositions 64.5 wt% Co, 35.5 wt% MM and 27.0 wt% Co, 73 wt% MM respectively, were prepared by arc melting. The latter is sintering additive (melting point 900°C).

Bulk material from both the MM Co_5 alloys and sintered additive was crushed separately to -100 mesh in pestle and mortar. Further reduction in particle size was achieved in a 600 ml attrition mill using petroleum ether as a milling medium. The two powders were finally blended in the mill to give a mixture containing 12.5 wt% of the sintering additive. The aimed composition of the mixtures was 59.8 wt% Co-40.2 wt% MM. Powders were aligned in a pulsed field of 50 k Oe, axially pressed to 2 k bar in the presence of a holding field of 7 k Oe and finally isostatically pressed to 7 k bar in the absence of a field, using rubber as the pressure transmitting medium. Further densification was achieved by sintering in a continuous stream of high-purity argon.

Prior to magnetic testing all samples were magnetised in a pulsed field of 50 k Oe (4000 k A/m).

Effect of process variables:

a) Milling time

Holding other conditions constant, the effect of varying the time during which the MM Co_5 material was milled, was examined. Powder properties after milling for 5,10,15,20 and 30 minutes are presented in Figure I.11. Compact properties after blending with the sintering additive, pressing and sintering for 1 hr at 1050°C to give around 95% of theoretical density are given in Figure I.12 and I.13. From Figure I.11, it is seen that as milling proceeded particle size decreased and $_JH_c$ increased. The results in Figures I.12 and I.13 show that in the case of powders milled for more than 10 minutes $_JH_c$ of the sintered compacts was greater than that of the powders and increased as milling time was increased. The optimum milling time in terms of B_r of the sintered compacts appears to be about 20 minutes, but the most square intrinsic demagnetisation curve (Figure I.13) and the highest value of $(BH)_{max}$ (8.0 MG Oe i.e. 64 k J/m^3) were obtained on a compact prepared from powder milled for only 15 minutes. It seems, therefore, that milling conditions are critical in that they influence the degree of squareness (or fulness) of the intrinsic demagnetisation curve.

b) Sintering temperature

The 15 minutes milled powders were blended with the sintering additive, compacted, and sintered for 1 hr at temperatures between 990 and 1110°C. Properties of the resulting

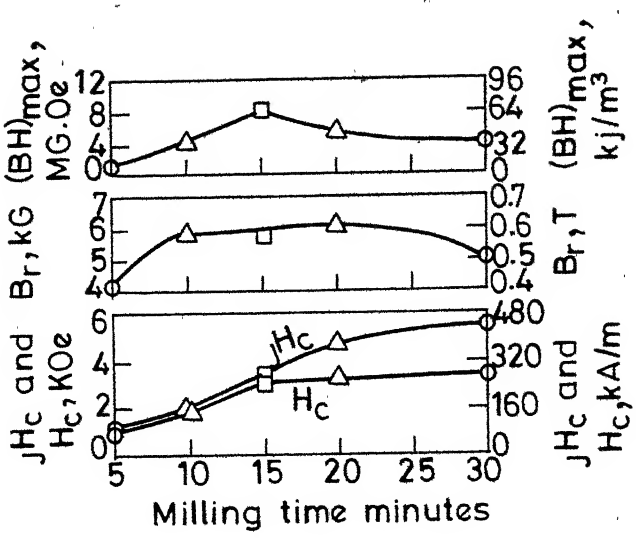

Fig.I.12 Effect of milling time on properties of compacts sintered for 1 hour at 1050°C. (Ref. 23)

- o Co 63.9 wt %
- △ Co 64.5 wt %
- □ Co 63.9 wt %

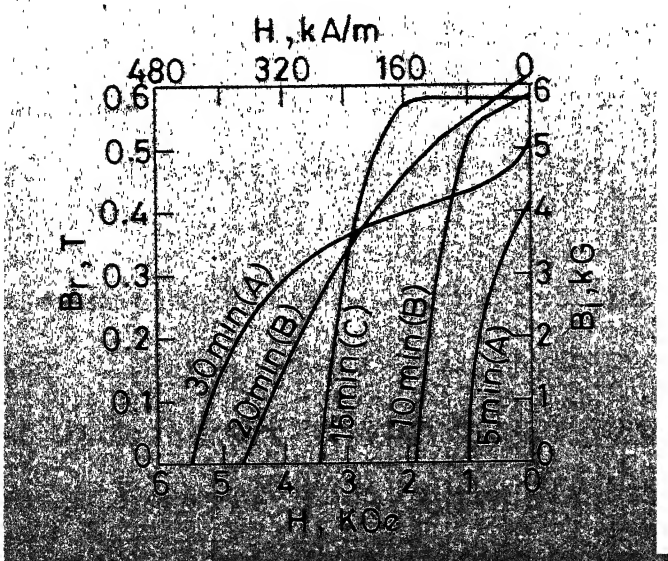

Fig.I.13 Intrinsic demagnetization curves for compacts prepared from powder milled for times between 5 and 30 minutes and sintered at 1050°C for 1 hour (Ref. 23)

samples are shown in Figure I.14. It is clear from Figure I.14 that in general $_{J}H_{c}$ decreases and density and B_{r} increases with increasing sintering temperature. H_{c}, which is essentially constant for sintering temperature upto about 1040°C, decreases similar to $_{J}H_{c}$ at high temperatures. Maximum $(BH)_{max}$ (18.8 MG Oe) is associated with intermediate values of B_{r} and $_{J}H_{c}$ at a sintering temperature of 1040°C.

c) Sintering time

Compacts were sintered for various times at 1040°C and 1010°C respectively. The results are shown in Figure I.15. In terms of $(BH)_{max}$ and B_{r} the effect of sintering time was more marked at the higher temperature, an optimum time between 1/2 and 1 hr being indicated. $_{J}H_{c}$ decreased at both temperatures as time was increased from 1/4 to 1/2 hr, but this property increased significantly at 1010°C when sintering was prolonged for 2 hrs.

So by examining several of the factors involved in the preparation of MM Co_{5} magnets, it has been possible to obtain samples with properties much better than those previously reported by these authors. Each of the parameters examined appears to be critical and since various other factors such as composition, compaction condition etc. may will be significant, it is likely that optimum conditions have not yet been established.

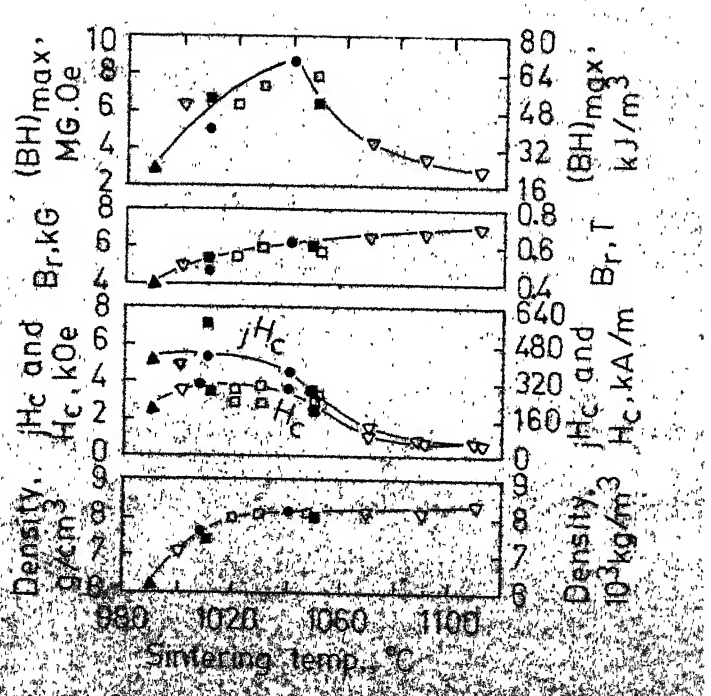

FIG. 1.14 EFFECT OF SINTERING TEMPERATURE (TIME : 1 HOUR) ON PROPERTIES OF $MMCo_5$ COMPACTS (REF. 23)

▽ Co 63.3 wt. % ▲ Co 64.4 wt. %
● Co 63.7 wt. % ■ Co 64.5 wt. %

1.3.4 Disadvantages of liquid phase sintering

Eventhough liquid phase sintering has many advantages, it has disadvantages too. Mixing should be proper. Otherwise compositional inhomogenity occur which is not preferred. Due to the liquid phase formed during sintering, shrinkage is also considerable. So dimensional accuracy is less. Liquid phase is more reactive, so chances for oxidation are more.

1.3.5 Sintering mechanism.

Gessinger et al[25] studied sintering kinetics of pre-alloyed and mixed powders to total Sm content between 33.8 and 40 wt%. The dimensional shrinkage of the compact was measured as a function of time and temperature. The rate exponent for the shrinkage was found to vary between 1/3 and 1/4. A rate exponent of 1/3 indicates grain boundary diffusion or diffusion rate controlled liquid phase sintering as the sintering mechanism. They suggest that, only simultaneous measurements of neck growth and shrinkage on well defined geometries can ascertain the operating diffusion mechanism. According to them concentration of cobalt vacancies increase with both time and temperature, because of the alloying of the additive and widening of Sm Co_5 homogenity range, and they suggest that the increase in Co vacancies would accelerate the diffusion process. From the above study they conclude that in both solid phase and liquid phase sinterings, sintering occurs mainly through solid state diffusion, though in the

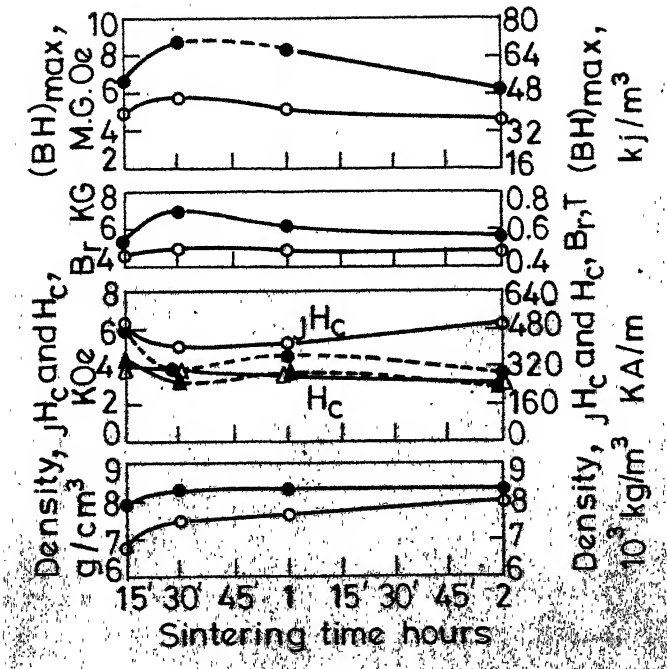

Fig. 1.15 Effect of sintering time on properties of $MMCo_5$ compacts. Milling time: 15 minutes. Sintering temp.: 1040°C (filled symbols) or 1010°C (open symbols) (Ref. 23)

Fig. I.16 Scanning electron micrograph showing islands of a Sm-rich phase at the free surface after heating a powder mix with 37 wt% total Sm content to 1170°C.(Ref. 25).

case of powder mixes the presence of liquid phase has been confirmed by electron micros copy. The liquid phase being rare earth rich serves simply as a supplier of Sm to the grains of base material.

The morphology of the sintered specimen was studied by scanning electron microscopy. In sintered powder mixes evidence for a liquid phase was found. While small amounts of a liquid phase can not be excluded in samples sintered at intermediate temperatures, a significant amount of a liquid phase must have been present in specimens sintered over 1120°C. The scanning electron micrograph shown in Figure I.16 is representative for all powder mixes sintered above 1120°C. It shows a distribution of small islands consisting of a Sm-rich phase, probably Sm_2O_3.

I.3.6 Summary:

Permanent magnetic properties of R-Co magnets depend on composition, pressing procedure, method of preparation, sintering parameters etc. Table I.6 shows the summary of the magnetic properties of R-Co magnets prepared by various methods.

Table I.6

S.No.	Composition	Method of Preparation	Magnetic Properties	Author and reference no.
1	$SmCo_5$	Pressed using binder	$(BH)_{max}$=8.1 MGOe	Buschow et al[6]
2	$SmCo_5$	Complex pressing process	$(BH)_{max}$=20 MGOe	Buschow et al[7]
3	$SmCo_5$	Isostatic pressing	$(BH)_{max}$=15 MGOe	Umebayashi and Fuzimura[8]
4	$SmCo_5$	Solid phase sintering	$(BH)_{max}$=16-20 MG Oe $_BH_c$ = 8-9 k Oe B_r = 8-9 k G	Das[9]
5	$Sm_xMM_{1-x}Co_5$	SPS	$(BH)_{max}$=14.5-18 MG Oe $_iH_c$ = 9.24 k Oe	Nagel and Menth[12]
6	$(Sm,MM)Co_5$	SPS	$(BH)_{max}$=14-15 MG Oe	Ratnam and Wells[13]
7	Sm-Co-Cu-Fe-Zr	SPS	$(BH)_{max}$=30 MGOe	Ujima et al[26]
8	Sm-Co	Liquid phase sintering	$(BH)_{max}$=15.7 MG Oe B_r = 8.06 k G	Benz and Martin[14]
		LPS with improved packing and alignment	$_BH_c$ = 7.7 k Oe $(BH)_{max}$= 20MG Oe	
9	Sm-Co	LPS	$(BH)_{max}$=18.0MG Oe H_c = 8.6 k Oe B_r = 8.6 k G	Shibata and Katayama[15]
10	Sm-Co	LPS	$(BH)_{max}$=18.4 MG Oe	Johnson and Fellows[16]
11	Sm-Co	LPS	$(BH)_{max}$=24 Mg Oe	Fonel et al[24]

(continued)....

Table I.6 (continued):

S.No.	Composition	Method of Preparation	Magnetic Properties	Author and reference no.
12	Sm-Co	LPS (in H_2 atmosphere)	$(BH)_{max}$=21.6MGOe B_r = 9.5 k G H_c = 9.13 k Oe	Jones et al[27]
13	Pr-Co	LPS	$(BH)_{max}$=16.6MGOe B_r = 8.53 k G $_MH_c$= 5.54 k Oe $_BH_c$= 4.98 k Oe	Tusi and Strnat[17]
	Pr-Sm-Co	LPS	$(BH)_{max}$=21.1MGOe B_r = 9.21 K G $_MH_c$ =12.67k Oe $_BH_c$ = 7.14 k Oe	
14	Sm-Pr-Co	LPS	$(BH)_{max}$=20MGOe $_iH_c$ = 10.6 k Oe B_r = 9.7 k G	Shibata and Katayama[15]
15	Sm-Pr-Co	LPS	$(BH)_{max}$=26 MG Oe B_r = 10.26 k G $_BH_c$ = 10.13 k Oe	Benz and Martin[19]
16	Sm-Pr-Co (0.5% Fe_2Sn additive)	LPS	$(BH)_{max}$=25.5MGOe B_r = 10.45 k G $_BH_c$= 9.75 k Oe	Hou-ting[28]
17	MM-Sm-Co	LPS	$(BH)_{max}$=20MGOe	Benz and Martin[21]
18	MM Co_5	Isostatic pressing	$(BH)_{max}$=3.1MGOe	Mc.Caig[22]
19	MM-Co	LPS	$(BH)_{max}$=4.4MGOe	Johnson and Fellows[16]
	MM-Sm-Co	LPS	$(BH)_{max}$=10.6MGOe	
20	MM-Co	LPS	$(BH)_{max}$=18.8MGOe	Johnson and Fellows[23]

II. STATEMENT OF THE PROBLEM

The discussion presented in the previous chapter shows that the misch metal-cobalt magnets prepared by liquid phase sintering have potential permanent magnet capabilities from the point of view of their properties. To take full advantage of the properties of these sintered magnets it is necessary to have a clear understanding of the effect of various process parameters on their properties.

Indian misch metal, containing some iron and other impurities, is used in this study. Obviously, process parameters will have to be optimized when sintering technique is applied to Indian MM-Co alloy.

In the present work, it is therefore proposed to investigate the following parameters as they affect magnetic properties of MM-Co sintered magnets:

1) Milling time in different comminution processes such as ball milling, rod milling and E M pulveriser.
2) Composition
3) Compaction pressure applied during field-pressing and effect of field pressing process.
4) Sintering temperature and time
5) Temperature and time of annealing of sintered pellets.

The experimental tools to be employed for characterization include: X-ray diffraction, metallography, Fisher

Sub-sieve analyser, optical microscopy, and a vibrating sample magnetometer with a gauss meter for magnetic measurements.

III. EXPERIMENTAL TECHNIQUES

The whole process involved in the present study on liquid phase sintering of MM-Co alloys is depicted in Figure III.1. In the following pages each of these steps is elaborated.

III.1. Starting materials

The starting materials used for the preparation of MM-Co alloys (base material and additive) are misch metal, supplied by Mischmetal and Flints Pvt. Ltd., Allepey, Kerala and 100% pure cobalt.

The composition of misch metal was found to be 91% RE, 6% Fe and 3% other impurities.[29] Cobalt was 100% pure.

III.2. Compositions

III.2.1. Calculation of the eff. gm. at. wt. of rare earths

Since the exact rare earth composition of MM was not known the average of the range supplied by the supplier for rare earth, was taken as the basis for the calculation of the effective gram atomic weight of rare earths. This calculation is given in Table III.1.

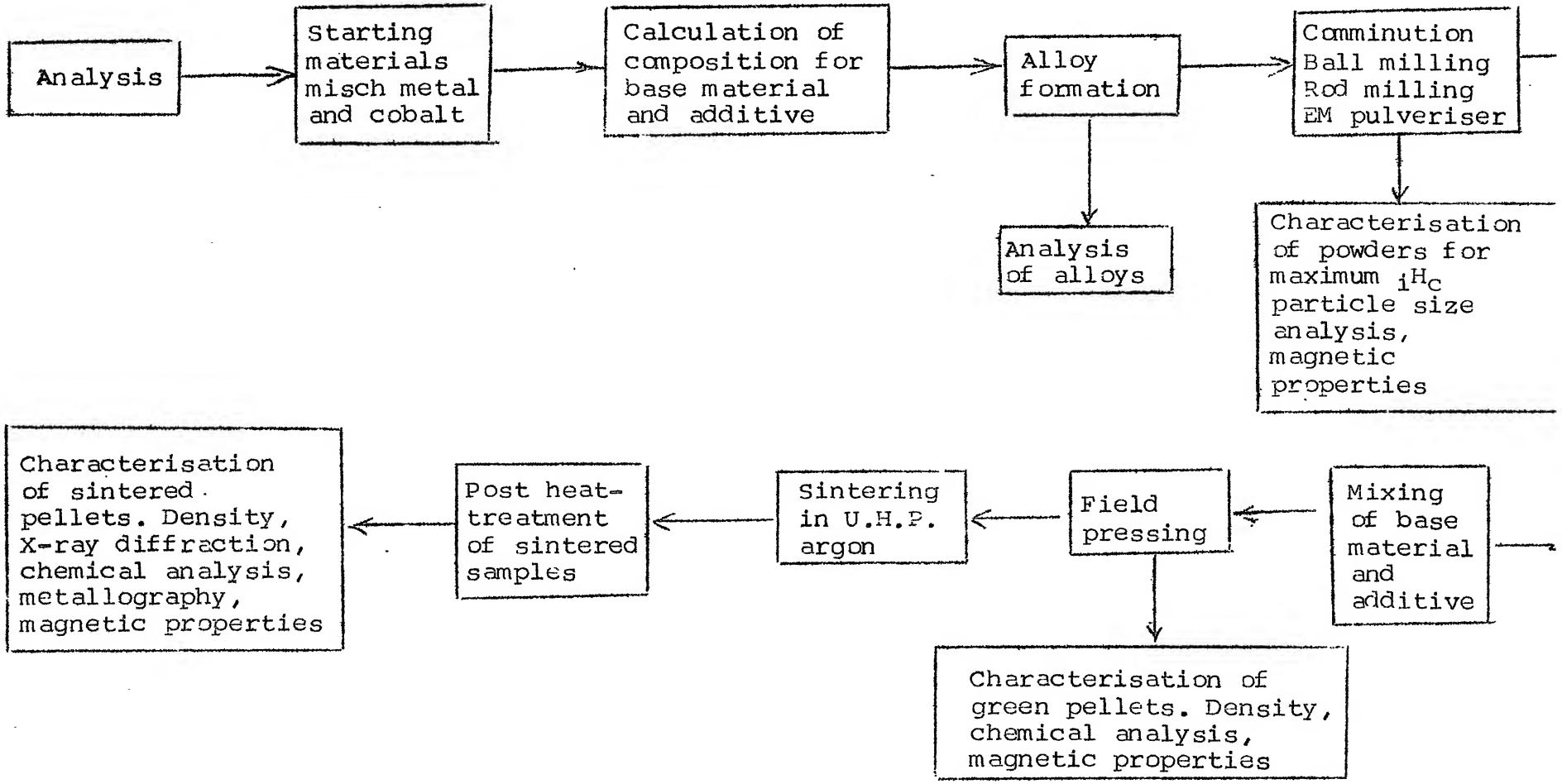

Figure III.1. Block diagram of the liquid phase sintering of MM-Co alloys.

Table III.1. Calculation of effective gr. at. wt. of rare earths.

Element	Ave. wt. Pct.	At. wt.	Contribution by individual RE elements to gr. at. wt. of RE
Ce	47.5	140.12	0.475 x 140.12 = 66.56
La	22.5	138.91	0.225 x 138.91 = 31.25
Nd	17.5	144.24	0.175 x 144.24 = 25.24
Pr	5.0	140.91	0.050 x 140.91 = 7.05
Sm	2.5	150.35	0.025 x 150.35 = 3.76
Y	1.5	88.91	0.015 x 88.91 = 1.33
Total	96.5		135.19

$$\text{Eff. gr. at. wt. of RE} = \frac{135.19}{96.5} \times 100$$

$$= 140.09 \text{ gms.}$$

III.2.2. Calculation of composition

a) Base material:

The Fe present in misch metal was assumed to replace a part of cobalt. On the basis of this, the composition of the base material can be represented as

$$MM\ Co_{5\pm y} = RE\ (Co_{1-x}\ Fe_x)_{5\pm y}$$

The base material composition aimed at was 35.5 wt. percent RE and 64.5 wt. percent (Co + Fe). The same composition was chosen by Johnson et al.[2]

Our MM contains 91% RE.

So MM needed to get 35.5 grs. of RE $= \frac{35.5}{91} \times 100$

$= 39.01$ gms.

39.01 gms. of MM gives $\frac{39.01 \times 6}{100} = 2.34$ gms. of Fe

Cobalt needed $= 100 - (35.50 + 2.34)$ or $(64.5 - 2.34)$

$= 62.16$ gms.

So to get 100 gms. of (RE + Co + Fe), the MM to be taken is 39.01 gms. and Co of 62.16 i.e. total of 101.17 gms. This extra 1.17 gms. are impurities in MM and assumed that they do not react with RE, Co or Fe.

Now, percentage of MM $= \frac{39.01}{101.17} \times 100$

$= 38.55$

Percentage of cobalt $= 61.45$

∴ Composition of base material is 38.55% MM and 61.45 wt.% Co. When written in the form of $RE(Co_{1-x}\ Fe_x)_{5\pm y}$, the base material has the molecular composition of $RE(Co_{0.96}\ Fe_{0.04})_{4.33}$.

b) Additive material:

The composition of additive material aimed at is 73 wt. % RE and 27 wt. % Co. When calculated in a similar way, this comes to 78.33 wt. % MM and 21.67 wt. % Co.

Table III.2. Starting compositions

Alloy	wts. taken		Actual amounts of pure elements					
	MM	Co	RE	Co	Fe	Co+Fe	Total	Balance
Base material	38.55	61.45	35.08	61.45	2.31	63.76	98.84	1.16
Additive	78.33	21.67	71.28	21.67	4.70	26.37	97.65	2.35

The balances are the impurities coming from misch metal.

III.3. Alloy formation

III.3.1. Materials preparation

The misch metal supplied was in the form of ingots coated with grease to prevent them from atmospheric oxidation. The ingots were cut into small pieces of about 1 cm^3 in volume. The pieces were washed with acetone to remove the grease coating. All surfaces of these pieces were ground to remove any oxide layer present. The pieces were stored under toluene to prevent oxidation until they were weighed and used for melting.

Cobalt was in the form of flakes. These flakes were washed with acetone to remove any dust or greasy particles sticking to their surface. Surfaces of these pieces were ground when necessary.

Before melting, the required amounts of misch metal and cobalt were weighed to ~~a~~ an accuracy of 0.001 gms.

III.3.2. Arc melting

Base material and additive in the present study were prepared by arc melting.

The d.c. arc melting unit consists of a water cooled copper crucible and a non-consumable tungsten electrode. Usually currents of 300-600 A at voltages 30-45 V were used for melting.

The copper crucible was polished with an emery paper and degreased with acetone. Some times a small amount of alloy got welded to the copper crucible during melting and this was removed by using a hand-grinder. The MM and Co pieces were arranged such that the MM was always under cobalt pieces. The furnace chamber was evacuated using a rotary pump to 30-40 microns, flushed thrice with ultra high purity argon and finally filled with argon. In some cases, commercial argon was used and in that case, it was purified using a gas purification system. The arc was always struck between the electrode and cobalt. A duration of 30 seconds was used for each melting. For proper homogenization each alloy was remelted thrice after breaking and putting it upside down every time.

The arc-melted alloy buttons were very brittle and broke in the crucible by themselves due to chilling action of the water-cooled copper crucible. The shiny pieces were stored in dessicator. The weight losses during melting were found to be less than 0.5%. Usually 40-50 gms. of material was melted each time.

The observed weight losses may be due to (i) smallest particles which were formed during breaking of the alloy button might have escaped from being collected and (ii) due to the evaporation of the low melting misch metal because of uncontrollable arc temperature.

III.4. Comminution

III.4.1. Crushing

The as-cast alloy buttons were crushed using a tool steel crusher. The crushed powder was sieved with 160 microns sieve by using Fritsch Laboratory Sieve Shaker and -160 microns powder was used for ball milling and rod milling.

III.4.2. Ball milling

As large amounts of powders were needed for our study, more than 100 gms. of powder was milled in ball milling each time. Two ball milling experiments were carried out, one with plastic container and the other with stainless steel jar.

The plastic container has approximately one litre volume and to get the required r.p.m. with this jar, sponge was placed between the plastic container and an outer ceramic jar. The latter rotates on the bars of ball mill. The plastic container rotates along its axis. Stainless steel balls of 12 mm. dia. were used. The grinding was always done under toluene - a protective liquid medium.

Before using stainless steel jar for the second ball milling experiment, the same plastic container was tried. In this case no sponge was put and the plastic container was allowed to rotate in the outer jar. But due to the reaction of toluene with the plastic container, the shape of the plastic

container got distorted and it was sliding in the jar. So the r.p.m. became less. To avoid this difficulty, stainless steel jar was used in the second case.

For this purpose, a stainless steel tube (non-magnetic) of 3½" outer diameter, 1/8" thick and 6" length was taken and one of its ends was welded with circular stainless steel plate. The other end was provided with a threaded lid. An 'O' ring was provided in between these two to avoid leakage. Rubber bands were wrapped on the outer surface of the stainless steel jar to provide friction between the stainless steel jar and the outer ceramic jar, to reduce noise and to avoid damage to the outer ceramic jar. Effective height of this jar is approximately 14 cm.

III.4.3. Rod milling

In our efforts to get high $_iH_c$ value for base material powder, we also tried rod milling besides ball milling. For this purpose, the stainless steel jar used in ball milling, was used. Non-magnetic stainless steel rods of 1/8" diameter and 13 cm. length were used as grinding medium.

Before each milling, the stainless steel jar and the grinding medium were cleaned first with dilute nitric acid (which dissolved the MM-Co powder sticking to their surface) and then with water. Then, they were thoroughly dried and used for grinding.

After milling, the powder was extracted and stored in toluene/vacuum dessicator to prevent oxidation.

III.4.4. E M pulveriser

Fritsch electromagnetic laboratory micropulveriser was also used for comminution of base material besides milling. This electromagnetic-powered mortar generates vertical oscillations which are transmitted into the grinding ball across the grinding stock. The impacting energy of the grinding ball is controlled by a rotary rheostat. The utilisation of a grinding ball with an even heavier unit weight will increase the impacting efficiency.

The coarse grain constituent is, during the initial operating phase, selectively crushed and reduced in size. With the grain size range gradually reducing, the grinding ball begins to tumble inside the mortar. This provides for a grating effect resulting in uniform fine grinding and mixing/homogenising of the sample.

The amplitude of oscillations can be set steplessly. In the experiments conducted it was set at 6.5 (on a scale of 1-10) and 3000 oscillations per minute were given by setting the knob to 'perm' position. The amount of material used was 10 gms. and liquid paraffine was used as a protective medium as toluene affects the plexiglass viewing window. Steel ball was used for grinding purpose, to have higher impacting efficiency.

III.5. Mixing of base material and additive

Homogeneous mixing of base material and additive powders is very important. Otherwise there will be composition gradients, differential shrinkage etc.

Before weighing these two powders, they were completely dried in vacuum dessicator. If there is any toluene left in the powder, there will be an error in getting a particular nominal composition of the mixed powder. This was checked by absence of continuous weight loss (due to the evaporation of toluene, if present) during weighing. They were weighed to an accuracy of 0.001 gms. in the required amounts. As soon as they were weighed, they were stored in toluene to avoid oxidation.

First both were mixed thoroughly in a mortar in toluene medium. After that they were further mixed by rod mill for 30 minutes in toluene (care was taken to avoid loss of powder by flying off or by sticking to the walls during mixing). After mixing the powder was dried and pressed into pellets.

III.6. Pressing

The first step in densification process is pressing the powder into green pellets. This is achieved in two stages. First is field pressing and the next is hydraulic pressing. Field pressing was done by two methods. 1) Field pressing

by a screw type brass assembly in steady magnetic field of an electromagnet and further pressing by hydraulic press to increase density and 2) using RFL pulse magnetiser combined with 20 T Bemco hydraulic press. In this, magnetic field application and pressing are done simultaneously in a single step. The purpose of field pressing is to orient the powders when they are being pressed.

III.6.1. Field pressing using brass assembly

A schematic sketch of this field-pressing apparatus is given in Figure III.2. This is made of brass. Non-magnetic plungers were used to prevent any magnetic attraction between the pellet and plungers, the presence of which might cause damage to the pellet. The die part is also made of non-magnetic steel.

Before starting, the plungers and die were cleaned with acetone. First, one handle was screwed to the assembly and one plunger (smaller one) was inserted into the die. The weighed powder ($\simeq$1.2 gms.) was poured in the die by using a funnel. No binder was added to the powder. After that, the other plunger was inserted and then the second handle was inserted. The entire assembly was placed inside the magnet in such a way that the middle part of the die, which contained the powder was lying in between the two pole pieces. In this position, the applied field will be along a diameter of the pellet i.e. perpendicular to the height of the pellet.

magnetic field was gradually increased to 15k Oe, then the powder was pressed by slowly rotating the handles and thereby pushing the plungers on both sides towards each other. The maximum possible pressure was used during this operation. In this device, it is not possible to estimate the pressure applied.

The pellets which were field pressed as above were densified further by hydraulic pressing. A single action hydraulic press of maximum load capacity of 24,000 lbs was used for this purpose. A split die and plungers made of die-steel were used. The field pressed pellet was placed in the die. Eventhough the capacity of this hydraulic press is 24,000 lbs, it could only go upto 15,000 lbs. This has put a limit on the maximum pressure at 1,36,600 psi (diameter of plungers is 0.95 cm) green density of the pellet was found after hydraulic pressing. Three different pressures were used in the present study.

III.6.2. Field pressing using pulse magnetiser

Field pressing apparatus using a pulsed field magnetiser contains three units. 1) Pulse field magnetiser, 2) fixture and 3) hydraulic press. RFL model 747-6 magnet charger, RFL charging fixture and Bemco hydraulic press were used for this purpose.

The RFL model 747-6 magnet charger is a capacitor discharge device designed for high stored-energy levels with

lower power demand on the input power source. The EMF applied to charge capacitor banks in each energy capacity level is continuously variable upto 400 VDC. The energy-capacity level for 747-6 is 6,000 Joule at 400 V. Energy-storage-bank restoring times are dependent upon the level of the applied EMF selected and the level of the A.C.-input power used.

RFL charging fixture is essentially a solenoid with the dimensions of 3½" inner dia, 2" thick and 2" length. This is fixed on the platform of hydraulic press and is connected to the magnetiser. Bemco hydraulic press has a capacity of 20 tonnes and can be operated manually or automatically.

To carry the field pressing operation, bottom plunger is lowered and the powder is poured into the die. Pressing operation and magnetiser operation timings are sychronised such that the pulse is released during the pressing of powder.

III.7. Sintering in inert gas

The pellets were sintered in a continuous flow of ultra high purity argon gas. This was done in a vacuum-cum-inert atmosphere furnace.

III.7.1. Sintering furnace (vacuum-cum-inert atmosphere)

The design of the furnace is shown in Figure III.3. This is a tube furnace and heating element is wound on this tube. The construction details are clearly discussed by

Table III.3. Parts of the furnace

Sr. No.	Description
Z	Power terminals
Y,Y'	Brass flanges
X	Vacuum pump connecting tube
W	Argon inlet valve
V	Pt-Pt-Rh-thermocouple leads
U	Thermocouple sheath
T	Black wax sealant
S	Aluminium shell
R	Kanthal winding
Q	Stainless steel supporting rod
P	Magnesia-asbestos powder
O	Alumina cement on winding
N	Quartz boat
M	Furnace tube (Mullite)
L	Cement-asbestos sheets
K	Silicone rubber sealant
J	Radiation shields (S.S.)
I	Radiation shield support (Copper tube)
H	Neoprene 'O'-rings
G	Extension brass fitting
F	Pulling rod (S.S)
E	Special vacuum valve
D	Brass couplings
C,C'	Mullite tubes
B	Copper cooling coils
A	Extension sleeve

Shankara Prasad.[30] This can go upto 1150°C. Parts of the furnace are given in Table III.3.

III.7.2. Sintering furnace operation

The water connections are made and continuous circulation was ensured. The furnace is slowly heated, taking about 5-6 hours to reach the required temperatures between 1000-1100°C. Under these conditions, about 8 amperes current flows at 165 volts. The pressed pellets are arranged in a fused silica boat. The boat is hooked carefully on to the pushing rod, and then introduced into the furnace at the cooled end of tube C'. Now the boat is in the cooled zone. The brass flanges are tightened. All the vacuum fittings are greased with silicone grease, before evacuation.

The furnace is evacuated using a rotary pump. When the vacuum reached a value of approximately 100 microns, the pump is stopped and the furnace is flushed with argon. The furnace is evacuated and is refilled with argon . After flushing three times with argon, argon is continuously passed and flow is controlled at 2-3 bubbles per second.

Now the boat is pushed to centre of the furnace slowly taking about 30 minutes to reach the centre. When the boat is at the centre of furnace the time is noted and thus sintering is carried on for the required time.

After the sintering is over the boat is pulled back to the room temperature zone. The argon flow rate is increased

slightly to enhance the cooling rate. It has been found that it takes about 20-25 minutes for the pellets to come down to room temperature. Then they are taken out of the furnace Using the above mentioned inert atmosphere sintering furnace, sintering experiments were done to study the effect of different variables, on the permanent magnetic properties and sintered density viz.:

a) sintering temperature in the range 1000°C to 1100°C.

b) sintering times of 30 and 60 minutes duration.

c) nominal composition of the mixed powder.

d) applied pressure of the pellets in the range of 64,000 psi to 1,37,000 psi.

III.8. Characterisation

The as-cast alloys, powders, green pellets and sintered samples were characterised by various techniques shown below:

	As-cast	Powders	Green pellets	Sintered samples
Density measurements	X		X	X
X-ray diffraction	X			X
Metallography	X			X
Chemical analysis	X	X	X	X
Particle size measurement		X		
Magnetic measurements		X	X	X

III.8.1. Density measurements

Density and bulk density of as-cast and sintered samples are measured by the standard Archimedes liquid displacement method with toluene as the liquid. For this purpose, a small piece of the sample was weighed and boiled in toluene in a beaker for few minutes. After that, the beaker was put in a vacuum dessicator. This helps toluene to enter the pores more effectively. This piece was then weighed in toluene medium with the help of a wire. The piece was taken out of toluene and the toluene sticking to the surface was removed by a tissue paper and then immediately weighed. This includes the weight of toluene in the pores. From these data, density, bulk density and porosity were calculated as follows:

Example:

Weight of the sample in air w_1 = 1.1800 gms.

Weight of the sample in toluene w_2 = 1.0550 gms.
(wt. of the wire was taken into consideration)

Weight of the sample in air + weight of toluene in pores

w_3 = 1.1875 gms.

Specific gravity of toluene = 0.863 gm/cc

$$\text{True volume of the sample} = \frac{w_1 - w_2}{\rho} = \frac{1.1800 - 1.0550}{0.863}$$

$$= 0.1448 \text{ cm}^3$$

$$\therefore \text{ density} = \frac{1.1800}{0.1448} = 8.15 \text{ gm/cm}^3$$

$$\text{Pore volume} = \frac{W_3 - W_1}{\rho} = \frac{1.1875 - 1.1800}{0.863}$$

$$= 0.0087 \text{ cm}^3$$

$$\text{Bulk volume} = 0.1448 + 0.0087 = 0.1535 \text{ cm}^3$$

$$\therefore \quad \text{Porosity} = \frac{0.0087}{0.1535} \times 100 = 5.67\%$$

$$\therefore \quad \text{Bulk density} = \frac{1.1800}{0.1535} = 7.69 \text{ gm/cc}$$

$$\text{Relative density} = \frac{7.69}{8.15} \times 100 = 94.36\%$$

To find out the bulk density of the green pellet after hydraulic pressing, the sample was weighed, and diameter and height were measured by screw gauge. From weight and bulk volume, bulk density was calculated.

III.8.2. X-ray diffraction

GE-XRD-6 diffractometer was employed for X-ray studies of as-cast and sintered samples. The various settings used with the diffractometer are listed in Table III.4. X-ray patterns were obtained on -36 microns powders or sintered discs. Sintered discs were located in the sample holder using a screw arrangement. The surface exposed to X-ray was ground to remove the surface layer, in order that any surface contamination such as an oxide coating, does not interfere with the result.

Table III.4. GE-XRD-6 diffractometer settings

Radiation	Cobalt-Fe filtered
Tube voltage	50 KV
Current	5 mA
Scanning speed	2°/minute
Chart speed	1"/minute
Intensity range	200 CPS
Intensity plot	Linear
TC	2
Angular range scanned	30°-100°

III.8.3. Metallography

Microstructural study was carried out to supplement the phase identification done by X-ray diffraction for as-cast and sintered samples.

The samples for microstructure were prepared by grinding on emery papers (1/0, 2/0, 3/0 and 4/0) and finally lapping them on a polishing cloth with 0.1 micron alumina powder. A 2 percent nital etching for 2-3 seconds was sufficient to bring out the microstructure of as-cast alloys. A 'Carl Zeiss NU-2' microscope was used for the microstructural observation.

III.8.4. Chemical analysis

Chemical analysis was carried out to find out the amounts of total rare earths, Co and Fe by using complexometric titrations with EDTA. As cast and sintered samples were analysed to find out any variation of composition due to melting or sintering. Powder samples were analyzed to find out if any oxidation had occurred and to check out the homogeneity of mixed powders.

III.8.5. Particle size measurement

Particle size measurement of the base material powder was done by two methods:

1) Fisher sub-sieve analyser
2) Optical microscopic method

III.8.5.1. Fisher sub-sieve analyser

Fisher sub-sieve analyser is a simple and standard instrument used for measuring average particle diameter of the powder when it is in the range 1-50 microns. This does not give any information regarding particle size distribution. In this, air at constant pressure is passed through the bed of powder and resistance to the flow of this air is a measure of particle size. An amount of powder equal to its density is used in this experiment.

III.8.5.2. Optical microscopic method

Besides average particle size, particle size distribution can also be found out by this method. Particle size distribution is also one of the parameters which affect the $_iH_c$ of the powders. Optical microscopy is the most direct method. There are three distinct steps involved in characterising a powder by this method.

1) Slide preparation
2) Particle size measurement
3) Treatment of the data.

III.8.5.2.1. Slide preparation: The success of the microscopic method depends on whether the measured particles are representative of the bulk. This to a large extent, depends on how the slide was prepared.

About 0.05 gms. of powder was taken in a test tube and about 10 cc of acetone was added. In the present case the powder particles were heavy and had a tendency to settle down rapidly. In addition, as the particles were magnetic, they had a tendency to stick to each other. Just a hand shaking was not enough to disperse the particles. So ultrasonic vibrator was used for dispersing the particles. This gave a very good dispersion of particles and it was possible to maintain this dispersion for longer time without settling. The test tube was kept for about 30 seconds in an ultrasonic vibrator. After getting dispersion, 4-5 drops were dropped

on a clean ceramic tile. Care must be taken to see that one drop does not fall on the other. Instead of microslide, the ceramic tile gave good background, without any strains. The tile thus prepared was studied under microscope.

III.8.5.2.2. Particle size measurement: The particle diameters were measured with a 'Carl Zeiss-NU2' microscope using a calibrated Filar micrometer eye-piece. The procedure was clearly discussed by Subramanyam.[31]

The microscope settings used throughout this work are:

Eye-piece - 15 X

Objective - 63 X

Zoom lens dia. - 12.5

The eye-piece was calibrated for the above settings and it was found that each division on the spindle corresponds to 0.25 microns.

A total of 100 particles were measured from one ceramic tile for each powder in the present work.

III.8.5.2.3. Treatment of the data: The measured diameters were grouped into classes which were defined by means of particle size limits called class boundaries. The mid point of each interval was called the class mark and was denoted by d_i, where i was the number of the interval. The number of particles in each interval was called the frequency f_i, and the total number of particles measured was denoted by N.

The data classified as above was then represented in a graphical form by a histogram. In this plot the abscissa represents the diameter and the ordinate represents the frequency per class interval.

The average particle size was determined by calculating the arithematic mean $\bar{d}$ which is given by the equation.

$$\bar{d} = \frac{1}{N} \sum_{i=1}^{n} d_i f_i$$

where n is the number of class intervals.

III.8.6. Magnetic measurements

The following instruments were employed for the magnetic measurements.

1) Polytronic magnet type RTB-200 - for producing magnetic field as high as 12 k Oe.
2) Polytronic gauss meter type GM-502 - for measuring the fields.
3) Princeton Applied Research Vibrating Sample Magnetometer model 155 - for measuring magnetic moment.

III.8.6.1. Procedure for measuring saturation magnetisation, remanence and intrinsic coercivity

The combination of the three instruments mentioned above makes an excellent set up for measuring saturation magnetization, remanance and intrinsic coercivity.

The plastic bonded sample (preparation of this was clearly discussed by Subramanyam[31]) or green or sintered pellet (this is ground to the required size) was mounted into the sample holder of vibrating sample magnetometer with its direction of alignment parallel to the direction of the applied field. The position of the sample was adjusted using the 'saddle point adjustment' mechanism of the magnetometer such that it was in the centre of the field where the pickup coils are situated.

The field was increased to the maximum value (12 k Oe) which was sufficient to take the sample to saturation. The saturation magnetisation in e.m.u. was read from the digital display of the magnetometer. Then the field was brought to zero and the reading on the display was again taken down which gives the value of ramanence in e.m.u. Now the direction of the field was reversed. The demagnetizing field was increased slowly until the moment reading on the magnetometer was zero. The value of the field at which moment goes to zero is the value of coercivity and was measured with the help of the gauss meter. This is the step at which maximum care should be exercised in controlling the field. If the field is increased rapidly, there is every possibility of the value of moment crossing its zero value and going to the negative direction very fast. In such a fast transition, errors may be committed in reading the coercivity from the

gauss meter. Such error can be minimised to a large extent by making use of the fine control provided with the magnet power supply, when the moment is approaching zero.

The demagnetization curve of a good permanent magnet shows the following behaviour. As the reverse field is increased, the moment does not decrease initially very much from its remanance value. But as the coercivity value is approached it decreases quite rapidly, thus showing squareloop characteristic. The values of saturation magnetization and remanance, as they were read from the magnetometer, were in e.m.u. and to express them in standard notation of emu/g, they have to be divided by the weight of the powder present in the sample.

IV. RESULTS AND DISCUSSION

IV.1. Analysis of as-cast alloys

Weights of MM and Co taken and actual amounts of pure RE, Co and Fe for base material and additive were given in Table III.2. During arc melting the weight loss was found to be less than 0.5 percent. The base material and additive were analysed by chemical analysis and the results are given in Table IV.1. Intended amounts (values from Table III.2) are shown in brackets.

Table IV.1. Chemical analysis of starting alloys

Alloy	RE	Co	Fe	Co+Fe	Total
Base material	35.63 (35.08)	61.55 (61.45)	1.92 (2.31)	63.47 (63.76)	99.10 (98.84)
Additive	71.86 (71.28)	21.45 (21.67)	4.86 (4.70)	26.31 (26.37)	98.17 (97.65)

The percentage of (Co + Fe) were almost same but there was a small variation in RE content. This was attributed to the local variations in misch metal composition which varied from 90.21 percent to 91.92 percent RE from one corner to the other corner of the same piece.[29]

The base material was analyzed by X-ray diffraction method to find the phases present in it. The results are

Table IV.2. X-ray diffraction data of base material

Observed peaks			Standard peaks for the phases			
			1 : 5		5 :19	
2θ degrees	d (Å)	%I	d (Å)	%I	d (Å)	%I
35.40	2.9419	50	2.930	38		
36.63	2.8471	26			2.831	9
38.40	2.7194	19			2.714	13
42.10	2.4902	50	2.483	29		
48.70	2.1694	60			2.166	39
49.40	2.1405	86			2.134	100
50.00	2.1164	100	2.113	100		
52.40	2.0259	33			3.027	23
53.00	2.0046	38	2.003	19		
56.20	1.8990	16	1.898	17		
70.00	1.5594	24	1.562	16		
72.70	1.5091	24	1.509	14		
75.00	1.4693	17	1.468	21		
77.00	1.4368	12	1.437	5		
82.00	1.3634	19			1.364	26
82.40	1.3579	19				
82.80	1.3525	14	1.352	24		

given in Table IV.2 which clearly indicated the presence of 1:5 and 5:19 phases (in nearly equal proportion) which should be present according to the composition of the base material.

Microstructure of the as-cast alloy of base material at 1000X (Figure IV.1) shows 50 percent of 1:5 phase (dark) and 50 percent 5:19 phase (white) approximately, in agreement with the X-ray data.

X-ray and microstructural study of the additive alloy has been carried out.

IV.2. Comminution

In an effort to get high $_iH_c$ value for base material powder, two ball milling and two rod milling experiments were done. Out of these four experiments, for one ball milling experiment, plastic jar was used and the grinding conditions are different for this, whereas for the other three experiments, stainless steel jar was used.

IV.2.1. Ball milling

The optimum ball milling parameters for reducing the particle size are reputed to be[32]:

$$d/D = 0.05 \quad ; \quad J = 0.6$$

$$b/D = 0.001 \quad ; \quad f = 0.2$$

$$d^2/Db = 1.5 \quad ; \quad N/N_c = 0.6$$

Figure IV.1. Microstructure of base material showing 1:5 phase (dark) and 5:19 phase (bright) in equal proportion at 1000X.

where d is diameter of ball, D is diameter of Jar, b is size of feed, N_c is critical speed, N is actual speed, J is fraction of mill volume occupied by balls and space in between them and f is fraction of void space between balls which is occupied by solid particles.

The diameters of plastic jar and ball (stainless steel of density 7.9 g/cc) were 90 mm and 12 mm respectively. Ball diameter to jar diameter was 0.13 compared to an optimum value of 0.05. The number of balls added were 350 which made J = 0.55, close to the optimum value of 0.6. The critical speed of rotation (in r.p.m.) was calculated from the formula $54.2/(S - s)^{1/2}$, where S is the radius of the jar and s is the radius of the ball, both expressed in feet.[33] The critical speed was 152 r.p.m. from the above formula and 0.6 N_c is approximately 91 r.p.m. The speed of rotation was approximately 63 r.p.m. in this ball milling study. When the jar was filled with 350 balls, the void volume was 211 cc.

Optimum feed volume:

V_{op} = 0.2 x volume of space between the balls

= 0.2 x 211

= 42.2 cc

Tap density (using measuring jar) of the powder = 4 g/cm^3

So amount of powder to be taken = 4 x 42.2

= 168.8 gms.

Size of feed = - 100 mesh ($\approx$ 112.5 microns)

b/D = 0.00125

Volume of jar = 954 cc

wt. of balls = 2.5 kg

Volume of toluene added = 200 cc

After every grinding, an amount of powder ($\approx$ 9.0 gms.) required for particle size determination and H_c measurement was taken out and kept for drying in vacuum dessicator. The average particle diameter was determined by Fisher Sub-sieve Analyser. For this purpose, 8.43 gms. of material which is equal to its density, was necessary. This powder was exposed to air and air was passed through the bed of powder under pressure during particle size determination by Fisher Sub-sieve Analyser. As there would be some oxidation problem of this powder due to this, the powder was not added back after particle size determination. This decreased the amount of material in the jar after every grinding and there was steady decrease in f (upto 0.09) after every grinding.

Plastic bonded magnets were prepared with the powders after every grinding and $_iH_c$, M_r and M_s were measured and M_r/M_s was calculated. Table IV.3 shows these results.

Figure IV.2 shows the variation of average particle size, $_iH_c$ and M_r/M_s with milling time. The particle size decreased from 45 microns at 0.5 hours grinding to 2.4 microns

Table IV.3. Grinding time Vs. average particle size, $_iH_c$, $4\pi M_s$, $4\pi M_r$ and M_r/M_s

S.No.	Grinding time (Hours)	Average particle size (Microns)	$_iH_c$ (Oe)	$4\pi M_s$ emu/g	$4\pi M_r$ emu/g	M_r/M_s
1	0.5	45.0	100	67.8	30.5	0.45
2	2.5	11.5	550	75.9	46.4	0.61
3	4.5	7.6	700	77.0	53.7	0.70
4	6.5	6.2	810	71.6	52.8	0.74
5	8.5	5.3	890	75.5	59.4	0.79
6	12.5	4.5	1120	73.2	56.7	0.77
7	18.5	3.6	1300	83.5	64.1	0.77
8	24.5	3.2	1500	70.5	58.0	0.82
9	30.5	2.7	1450	71.5	57.7	0.81
10	37.0	2.4	1550	67.4	54.4	0.81

at 37 hours grinding hyperbolically. $_iH_c$ increased from 100 Oe at 0.5 hours to 1550 Oe at 37 hours. It can be expected after 37 hours grinding, $_iH_c$ will decrease as the curve became nearly very flat at 37 hours. M_r/M_s reached a maximum of 0.82 at 24.5 hours grinding and after that decreased slightly. M_s value varied between 67.8 and 83.5 (i.e. 20 percent variation) and the variation is not in a particular order. This value which is a property of the material should not change with particle size. This variation may be due to experimental error because the amount of powder in the plastic bonded magnet is determined by an indirect method. The binder and the resin used pick up moisture during the preparation of the magnet and this may give error in determining the amount of material. Also saddle point adjustment was not done every time, so this also may cause variation in M_s value.

It was not possible to grind further as there was not much material left in the jar due to taking away around 9.0 grams of material out after every grinding. The milling process was not very efficient in decreasing the particle size. There may be three possible reasons that may be contributing to this. 1) f was not maintained at 0.2 at all stages. After every grinding, f is decreased by 0.012 and when the stage of 37 hours grinding was reached, f was only 0.09 (approximately). 2) Spongy packing material was placed

in between the plastic jar and larger ceramic jar (so that r.p.m. of both the jars was 63). In this case, a part of the energy may have been absorbed by the cushioning action of the sponge. 3) The r.p.m. employed (63) is considerably less than 0.6 of the critical r.p.m. (91).

In the subsequent experiments f is maintained at constant value, no sponge material was placed in between the jars and 0.68 of critical r.p.m. was used. Because some reaction of toluene with plastic jar was observed, stainless steel jar was used in subsequent work.

With the above changes in experimental conditions, another ball milling experiment was carried out. The parameters are:

d/D	= 0.14	N/N_c	= 0.68
b/D	= 0.00125	f	= 0.18
J	= 55%	Amount of material	= 117 gms.

No. of balls used = 294.

Variation in $_iH_c$ value with grinding time for the above ball milling case is given in Table IV.4 and shown graphically in Figure IV.2. The value of $_iH_c$ increases with milling time reaching 1660 Oe for 36 hours and no over milling effect was found upto 36 hours. Over milling is the stage at which deterioration of $_iH_c$ value due to damage in the particles dominates the increase in $_iH_c$ due to reduction in the particle size.

Table IV.4. Grinding time Vs. $_iH_c$ value for ball milling of Figure IV.3.

S.No.	Milling time (Hours)	$_iH_c$ (Oe)
1	1	620
2	2	820
3	6	1180
4	13	1300
5	24	1450
6	36	1660

The shape of the variation of $_iH_c$ with grinding time is in agreement with that of other workers.[34-37] Table IV.5 shows the maximum $_iH_c$, milling time for getting maximum $_iH_c$ and composition of material used in these ball milling experiments.

From the Figure IV.2, it is clear that there is not much improvement in $_iH_c$ value in second case of milling even though ball milling parameters were maintained at optimum values mentioned above. Irrespective of the parameters the values are same which means the parameters mentioned above are not at all optimum. The reason for this may be that, the above optimum parameters were obtained using larger size jar, balls and feed. Also specific surface area per unit time was taken as a measure of the effectiveness of the grinding

Table IV.5. Maximum $_iH_c$, milling time and composition of material for various ball milling experiments.

Work of	$_iH_c$ (Oe)	Milling time (Hours)	Composition	Reference
Strnat et al	2600	30	$MMCo_5$	34
Strnat et al	2520	16	$MMCo_5$	35
Narita et al	2500	30	$MMCo_5$	36
	3500	16	$MMCo_{4.6}$	
	3000	14	$MMCo_{4.2}$	
	1500	8	$MMCo_{3.6}$	
Subramanyam	1025	-	$MMCo_{4.7}$	37
Present	1660	36	$MMCo_{4.3}$	

process which depends on particle size. But in the case of our ball millings, 3½" diameter jar was used which is smaller than the jar (20") that was used in obtaining the optimum parameters mentioned above. And also $_iH_c$ is a measure of the effectiveness of the grinding process which not only depends on particle size but also on damage caused to the powder. Larger the diameter of the jar, higher will be the impact energy on the particles and so higher will be the damage. So when damage is not taken into account the above optimum parameters may not be the optimum for our case in particular when jar size is comparatively very small.

Strnat et al[4] reported maximum $_iH_c$ of 2600 Oe for $MMCo_5$ at 30 hours grinding by using alumina jar of 2 litre capacity, large alumina cylinders (3/4" diameter by 1") and 45 grams of material. Each alumina cylinder weighs 30 gms. and total weight of grinding medium is around 600 gms. By using tool steel jar, of 2 litre capacity, smaller steel balls of 6 mm diameter (weight of each ball is 1 gm. and total weight is 2.8 kg) and 200 gms. of material, the same coercivity was achieved[35] at 16 hours grinding and it was still increasing slowly. In this case, d/D was reduced, volume filled by grinding medium increased and amount of feed increased. The slight improvement in the H_c may be due to the less weight of each steel ball compared to the alumina cylinder weight which causes reduction in damage and also the parameters may be near optimum values.

Narita et al[36] reported $_iH_c$ of 3500 Oe for $MMCo_{4.6}$ at 16 hours grinding. Milling details were not given and no reason was mentioned why $MMCo_5$ gave lower $_iH_c$ (2500 Oe) than $MMCo_{4.6}$. It was mentioned that peak $_iH_c$ can be obtained for shorter milling time with decreasing x (i.e. x in $MMCo_x$) and suggested that plastic deformation is introduced more easily and crystal is destroyed more extensively in the alloy x = 3.6 than alloy with x = 5.0.

The lower coercivity of 1660 Oe of the present work when compared to that of Strnat[34,35] et al and Navita et al[36] may be that the parameters are not optimum. And also it

was found in the chemical analysis of our powders that there is a decrease in RE and Co contents and increase in Fe contents and decrease in total RE + Co + Fe during milling. This also may be the reason for low $_iH_c$ values. The same reasons may apply to the values reported by Subramanyam.[31] These low values are not due to the impurities in RE as $MMCo_5$ produced from Flint MM and synthetic MM showed the same values of coercivity when both were rod milled under same conditions.[38]

IV.2.2. Rod milling

As there is not much information available for rod milling, parameters were taken arbitrarily. Table IV.6 shows the values of various parameters.

Table IV.6. Milling parameters in rod milling

Expt. No.	f	d/D	b/D	J	N/N_c	Amount of material ground (gms.)
1	0.20	0.0357	0.00125	0.52	0.72	80
2	0.13	0.0357	0.00125	0.52	0.72	52

Diameter of rods = 1/8"

Diameter of jar = 3½"

No. of rods used = 280

Particle size of feed = -160 microns

Composition of alloy = $MMCo_{4.33}$

Results of the above two cases are given in Table IV.7 and Figure IV.3. Ball milling curve of Figure IV.2 is also included for comparison. For rod milling, maximum $_iH_c$ is 1760 Oe for 28 hours for f = 0.20 and 1880 Oe for 24 hours for f = 0.13 and 'over milling' effect was found. For a given grinding time rod milled samples gave higher $_iH_c$ values than ball milled samples. At all grinding times magnetic properties are better for rod milling experiment with f = 0.13 than the same with f = 0.20. When the other parameters are fixed, f = 0.13 may be near optimum value compared to f = 0.20. This may be the reason for better magnetic properties for f = 0.13.

In ball milling or rod milling, as the grinding time increases, the average particle size decreases, particle size distribution becomes narrower and surface area increases (due to increase in surface area). In the initial stages of grinding most of the grinding energy will be spent in breaking the particles. This causes an increase in $_iH_c$. Also surface damage will be less due to low surface area. When particles become very fine, they coat on the grinding medium and cause cushioning action. Surface area will be more due to finer particles. If grinding is further continued, there will not be much reduction of particle size due to cushioning action and most of the grinding energy will be spent in increasing the surface damage of the powders. Also they get cold welded and form clusters which limit the $_iH_c$ value. $_iH_c$

Table IV.7. $_iH_c$ values at various grinding timings for rod milling.

f = 0.20			f = 0.13	
Time (Hours)	Particle size (Micron)	$_iH_c$ (Oe)	Time (Hours)	$_iH_c$ (Oe)
1	10.0	700	1	860
2	6.7	840	2	1100
4	5.4	1080		
6	4.7	1250	6	1560
10	3.7	1450		
14	3.1	1500	13	1700
20	2.5	1600		
26	2.3	1750	24	1800
36	2.1	1720	38	1620

depends on three factors. 1) Average particle size 2) particle size distribution and 3) damage in the powder. Ideally, fine, single sized powder having no damage will have maximum $_iH_c$. But this ideal situation cannot be achieved with any comminution process. One comminution process may improve one or more of the above three factors over the other processes.

Figure IV.4 shows the variation of $_iH_c$ with average particle size for ball milling (Figure IV.2) and rod milling (f = 0.20 in Figure IV.3). The average particle size was measured by Fisher Sub-sieve Analyser. In this analyser,

air flows through the bed of powder with a little pressure and so this may cause oxidation and thus lowering $_iH_c$ value. But 20 hours ground rod milled powder (f = 0.20) gave 1600 Oe of $_iH_c$ before and after measurement in Fisher Sub-sieve Analyser. So the oxidation due to this may be neglected.

It can be seen that, for the same average particle size, rod milled powder has higher $_iH_c$ than ball milled powder. The reason for this may be the difference in the particle size distribution. Rod mill produces a more closely sized product than the ball mill.[33] This is due to the preferential grinding of coarse particles over the fine particles in rod milling. Grinding mechanism in vibration milling and ball milling is different, but it is the same in rod milling and ball milling. So there will not be much difference in the damage introduced in the powder. But as more number of particles would be milled between two rods than the particles between two balls, the damage will be little less in rod milling when compared to ball milling.

Figure IV.5 shows the particle size distribution for ball milling (Figure IV.2) and rod milling (f = 0.13 of Figure IV.3) for 1 hour, 2 hours, 6 hours and 36 hours (38 hours for rod milling). They were measured by optical microscope and average particle sizes were calculated. It can be seen that rod milled powders have a narrower distribution and a lower average particle size than for ball milled powder. Both these factors together may be the

reason for higher $_iH_c$ for rod milled powders. If optimum parameters are determined and maintained, rod milling will have an edge over ball milling, due to a narrower particle size distribution.

IV.2.3. Chemical analysis of rod milled powders

To check the purity of the powder during rod milling, the powder was analysed by chemical analysis. Base material was ground by rod milling for 24 hours in toluene medium and sample is taken out and dried in vacuum dessicator. The chemical analysis of this sample before (i.e. as-cast) and after grinding is shown in Table IV.9.

Table IV.9. Chemical analysis of base material before and after 24 hours rod milling

	RE wt. %	Co wt. %	Fe wt. %	Total wt. %
As-cast	35.13	61.43	2.53	99.10
24 hours ground	33.07	58.12	4.45	95.64
Intended	35.08	61.45	2.31	98.84

The above table shows that there is deviation of chemical composition after rod milling. There is a decrease in RE and Co contents and an increase in Fe content. Total amount of (RE + Co + Fe) decreased from 99.10% to 95.64%. As-cast base material showed intended values and total of

RE + Co + Fe added to the correct amount. So some other element or elements other than RE, Co and Fe are coming into the powders during grinding. Fe may come into the powder during rod milling because of errosion of jar and rods. The other 3% cannot be Cr or Ni as they constitute only around 26% in stainless steel. To know about the deviation of chemical composition, some more experiments were done.

Base material was rod milled and samples were taken out at 1 hour, 6 hours and 24 hours for chemical analysis. Before closing the lid, air in the jar was flushed with argon. Moisture in the toluene if any was removed by using drierite. The chemical analysis results are shown in Table IV.10.

Table IV.10. Chemical analysis of base material after 1 hour, 6 hours and 24 hours of grinding

	RE wt. %	Co wt. %	Fe wt. %	Total wt. %
As-cast	35.44	60.69	2.56	98.69
1 hour	34.67	60.22	2.84	97.73
	34.53	60.20	2.84	97.57
6 hours	33.99	59.99	3.27	97.25
	34.04	60.05	3.29	97.38
24 hours	33.25	58.65	4.07	95.97
	33.44	58.52	4.09	96.05

The above table shows that as grinding time is increasing, RE and Co are decreasing, Fe increasing and total is coming

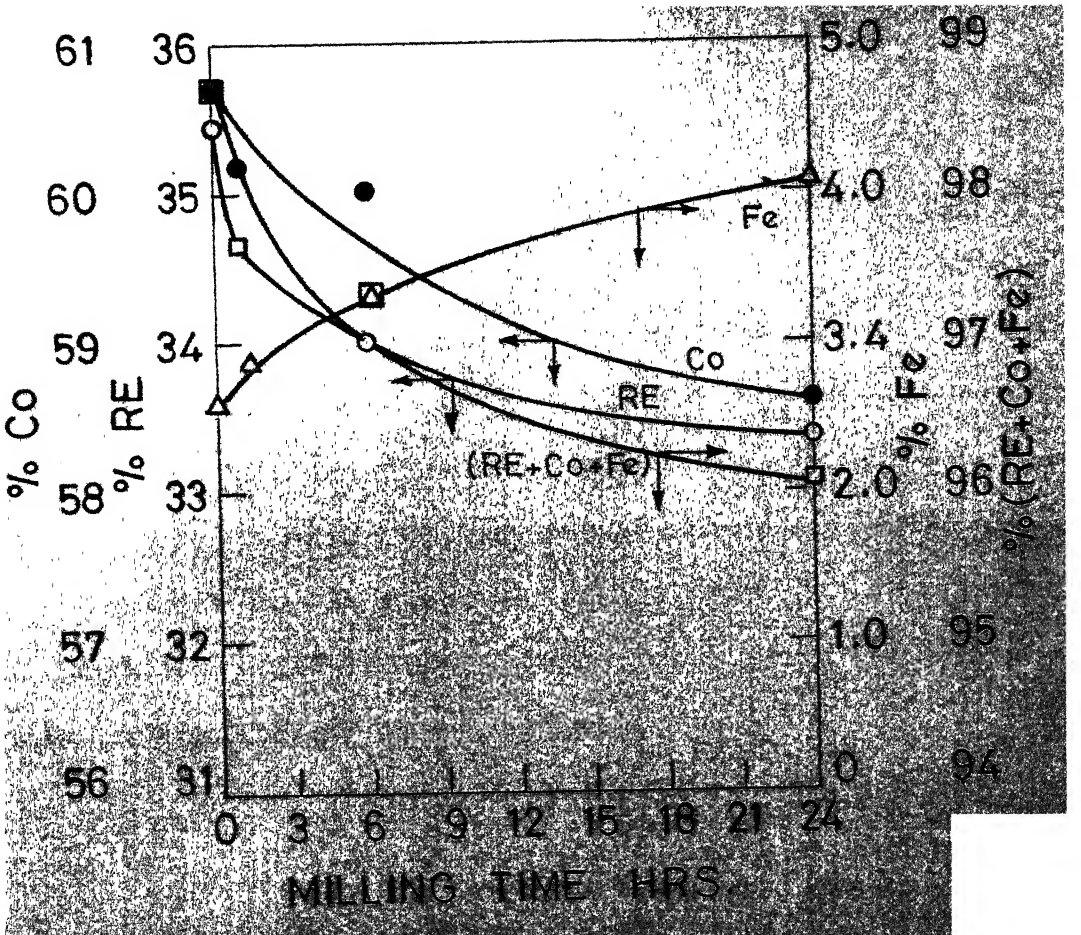

Fig.IV.7 Variation of wt % of Re, Co, Fe and (RE+Co+Fe) of rod milled powders with milling (ground in toluene medium)

down continuously. This is graphically shown in Figure IV.7. When these powders were dissolved in concentrated HNO_3 and diluted for chemical analysis, a small amount of undissolved matter or newly formed complex compound was observed. This residue is filtered and from visual observance, the amount of residue was found to increase with grinding time. The exact quantity of this residue was difficult to find out and it seems that this does not amount to 1-3%. To check whether this is coming from the jar, rods or toluene used, the following experiments were done: 1) Base material was rod milled without any liquid medium and samples were taken at 1 hour, 3 hours and 6 hours. 2) Base material was ground in small polythene jar for 24 hours and 3) Instead of toluene, acetone was used as liquid medium. Table IV.11 shows the chemical analysis results of these powders.

Table IV.11. Chemical analysis results of powders milled without liquid medium, acetone medium and in polythene bottle.

Sample		RE wt. %	Co wt. %	Fe wt. %	Total wt. %
Ground without liquid medium	1 hour	34.28	60.66	3.30	97.97
	3 hours	34.14	59.86	2.93	96.93
	6 hours	33.41	59.13	3.27	95.81
Polythene bottle, 24 hours		32.18	57.59	3.42	93.19
Acetone medium, 14 hours		30.63	55.00	4.84	90.47

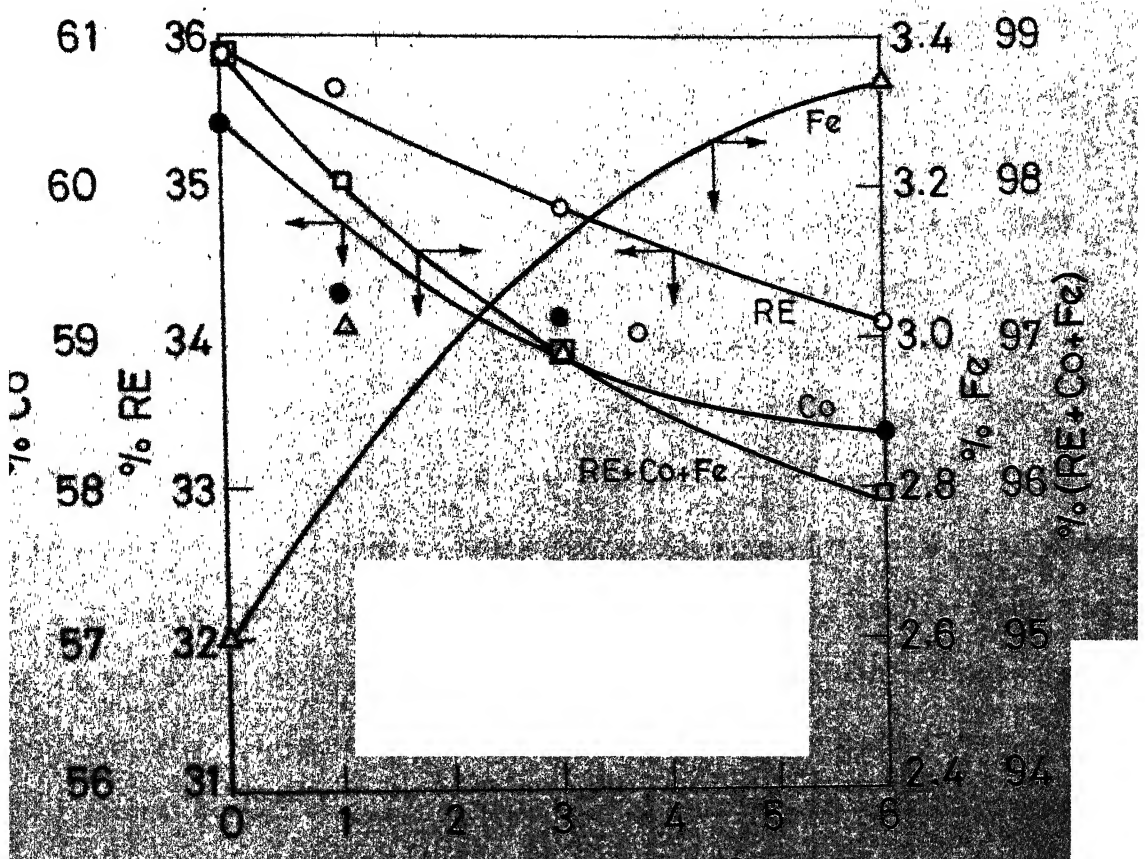

Fig. IV.8 Variation of wt % of RE, Co, Fe and (RE + Co + Fe) of rod milled powders with milling time ground without any liquid medium.

The Table IV.11 shows that there is again deviation from the chemical composition of as-cast material and for the powder ground with no liquid medium, the deviation increased with grinding time. This is graphically shown in Figure IV.8. All these powders left a small amount of undissolved matter during dissolution in concentrated HNO_3.

The above deviation from chemical composition from that of as-cast material in Tables IV.9, IV.10 and IV.11 is possible if there is any oxidation of the powders during milling, contamination of the powder due to toluene, rod milling jar and rods or if any complex compound which is difficult to dissolve forms during dissolution of the powder in concentrated HNO_3. The Fe pick up clearly shows that there is erosion of stainless steel jar and rods. But this cannot explain why the total of (RE + Co + Fe) is coming down. Stainless steel should completely dissolve in concentrated HNO_3 without leaving any residue. Contamination of the powders may not be due to toluene as, without using any toluene medium and using acetone as liquid medium gave the same results. Flushing the jar with argon before closing the lid will not remove the air in it completely and oxidation of powders is not ruled out. But only oxidation is not the reason for the above deviation as oxides of RE, Co and Fe should dissolve in concentrated HNO_3. As-cast material is not giving any complex compound which is difficult to dissolve during dissolution in concentrated HNO_3.

The chemical analysis of the powders was not reported previously. Purity of powders will definitely affect the magnetic properties of the powders and if this deviation from the chemical composition of as-cast material is avoided, there will be improvement in magnetic properties.

IV.2.4. Rod milling of additive material

When additive material was rod milled for 24 hours like base material, the powders were pyrophoric in nature because of the higher RE content and fineness of the powder. So additive material was rod milled for 6 hours. Coarseness of additive material will not have much effect during sintering as it will get melted during sintering.

IV.2.5 Electromagnetic pulveriser

The parameters that were used for grinding the base material by electromagnetic pulveriser are:

Feed size = -160 microns Amount of material used = 10 gms.

Amplitude = 6.5

Table IV.12 shows the average particle size measured Fisher Sub-sieve Analyser and $_iH_c$ values at different mes of grinding. The average particle diameter decreased th time continuously, but $_iH_c$ did not increase according the particle size. Visual observation after grinding owed that only a part of the material (material directly

Table IV.12. Grinding time Vs. average particle size and $_iH_c$

Time (minutes)	Particle size (microns)	$_iH_c$ (Oe)
15	46	320
30	43	690
45	35	520
60	26	620
90	23	400
120	20	640

below the steel ball) was ground very fine leaving the remaining without any grinding. Large and very fine particles (due to damage) will have lower coercivity and results cannot be conclusive. This is not suitable for mass production like ball mill and rod mill. Only 1-2 gms. can be ground to very fine size.

IV.3. Field pressing

Field pressing is to orient the powder when they are being pressed. This was done by using two methods: 1) using RFL pulse magnetiser combined with 20 T Bemco hydraulic press and 2) in the steady magnetic field of electromagnet using screw-type manual press made of brass and further pressing by hydraulic press. To compare the efficiency of the two processes in orienting the particles. Some field pressing experiments were carried out and magnetic properties measured.

Table IV.13 shows the magnetic properties of green pellets pressed by using brass assembly in steady magnetic field of 19 k Oe and the same sample further pressed in hydraulic press (load applied is 15,000 lbs). The powders used were base material rod milled for 24 hours. This table also shows the magnetic properties of plastic bonded magnet which is aligned in the presence of plastic fluid for approximately one minute at 11.0 k Oe and kept for setting for 24 hours. Plastic bonded magnet showed the same $_iH_c$ but higher M_s and M_r/M_s ratio than the field pressed samples in Table IV.13.

Table IV.13. Magnetic properties of green pellets, field pressed by using brass assembly and plastic bonded magnet.

Sample	$4\pi M_s$ emu/g	$4\pi M_r$ emu/g	M_r/M_s	$_iH_c$ Oe
Field pressed	52.06	31.26	0.60	2250
Field pressed + hydraulic pressed	54.57	32.05	0.62	2100
Plastic bonded magnet	73.06	53.88	0.74	2200

Table IV.14 shows the magnetic properties of green pellets pressed by using pulse magnetiser and hydraulic press. The load applied was 10 tonnes and pressing time was approximately 2 seconds. The magnetic pulse length is 100-200 milliseconds. Point 9 on the power level indicator (pointed upto 10) indicates a magnetic flux density of 13.3 KG inside

Table IV.14. Magnetic properties of green pellets pressed by using pulse magnetiser and hydraulic press.

S. No.	Approximate field	$4\pi M_s$	$4\pi M_r$	M_r/M_s	$_iH_c$
	KG	emu/g	emu/g	/	Oe
1	0	48.52	28.43	0.59	2050
2	4.5 (2 pulses)	45.59	23.14	0.51	2100
3	13.3	46.55	24.63	0.53	2100
4	13.3 (3 pulses)	48.92	25.98	0.53	2150

the die, and point 5 indicates 7.2 KG and point 3 indicates flux density of 4.5 KG. By using manual and automatic modes of hydraulic press, 1 to 3 magnetic pulses were given during pressing.

Table IV.14 shows that whether a magnetic pulse is given or not the magnetic properties seemed to be the same. Increasing number of pulses also did not improve the magnetic properties. Sample No. 3 is further magnetised in a pulsed field of different flux densities upto 60 KG, but did not show any effect.

In the Tables IV.13 and IV.14, $_iH_c$ values are same for all samples. But plastic bonded magnet shows higher M_s and M_r/M_s ratio than the other samples. The reason may be that when the magnetic field was applied, the particles were in plastic fluid and so they orient easily without much

resistance. And also they were aligned for longer time. In the case of samples pressed in steady field, field was applied while pressing was being done, so there may be resistance for the particle to orient easily and thus M_s and M_r/M_s were less than plastic bonded magnets. In the case of pulse magnetiser, whether the field was applied or not, the samples gave same values and M_s and M_r/M_s are less than the other two kinds of samples. Magnetic pulse was given at different stages during pressing to get the synchronisation of the pulse with pressing operation. This did not show any improvement. After field pressing the pellets are magnetic in nature which means powder is exposed to the magnetic field. The reason may be that the pulse length of 100-200 milli seconds may not be enough to orient the powders completely in the pressing time of 2 seconds.

IV.4. Liquid phase sintering

Some liquid phase sintering experiments were carried out for obtaining optimum composition, compacting pressure, sintering temperature and time for MM-Co magnets.

Table IV.15. shows the percentage of additive, total rare earth and Co + Fe in the three different compositions that were chosen for study.

After the pellets were field pressed, they were sintered in flowing argon atmosphere. Sintering was done at 1000°C, 1025°C, 1050°C and 1075°C for 30, 45 and 60 minutes.

ble IV.15. Amount of additive, total rare-earth and Co + Fe in mixed powders and starting powders (intended).

mposition of	Additive (wt. %)	RE (wt. %)	Co + Fe (wt. %)
ase material	-	35.63	63.47
dditive	-	73.10	26.00
1	5	37.50	61.60
2	10	39.38	59.72
3	15	41.25	57.85

The shape of sintered pellets got distorted and almost all pellets were found to have cracks. The top positions (in the boat) of the pellets have bigger diameter than the bottom positions.

In the hydraulic press (manual) that was used, the pressure is applied through the top plunger only. This causes density gradients along the axis which may cause differential shrinkage. If this is the reason for the distortion, after sintering top positions (in the hydraulic press should have bigger diameters because of higher density) than the bottom portions. But for some pellets top portions (in the hydraulic press) are bigger and for some pellets bottom portions are bigger after sintering. So differential density of the green density is not the reason for the distortion of the pellets. And also the green pellet thickness is around 2 mm and in this thickness, the density gradients may not be large. The

ellets pressess in Bemco hydraulic press in which the pressure is applied from top and bottom also showed the same distortion. If there are radial temperature gradients in the furnace, this type of distortion is possible.

Magnetic properties are found to be very low for all these sintered magnets. M_r/M_s is less than 20% and $_iH_c$ is between 60 and 620 Oe, RE-Co magnets should have permanent magnetic properties and these low values are not the characteristic values. MM-Co magnets are brittle in nature but these sintered pellets were found to be tough. These sintered magnets were analysed to find out the reason for these poor magnetic properties.

IV.4.1. Density

First some experiments were done after compacting field-pressed pellets at three different pressures. Sintered density was found to be slightly higher for 1,37,000 psi (which is maximum of three pressures) and less shrinkage compared to other pressures. This is due to the higher green density of the pellets. So in subsequent experiments only 1,37,000 psi pressure is used. Load applied at this pressure is 15,000 lbs. At this pressure, the green densities were between 5.4 and 5.7 g/cm^3. Bulk densities of the sintered pellets were found by liquid (toluene) displacement method. The bulk densities for all the three compositions at different sintering temperatures and times are given in Table IV.16.

Table IV.16. Bulk densities of the sintered magnets (in g/cc)

	Temperature — 1000°C		
Time —	30 minutes	45 minutes	60 minutes
C_1	7.31	7.51	7.50
C_2	7.35	7.52	7.50
C_3	7.38	7.38	7.26
	1025°C		
C_1	7.88	7.44	7.89
C_2	7.84	7.71	7.86
C_3	7.61	7.41	7.78
	1050°C		
C_1	8.06	7.73	7.86
C_2	7.97	7.50	8.06
C_3	7.60	7.63	7.63
	1075°C		
C_1	7.83	7.61	7.65
C_2	7.91	7.81	7.75
C_3	-	-	7.56

Minimum bulk density is 7.26 and maximum is 8.06 g/cc. For a particular composition, at a particular temperature, bulk density should increase with increasing sintering time. But this conclusion cannot be drawn from Table IV.16. The external cracks of the sintered pellets may be the reason for this. If there are external cracks, bulk densities will vary in a zig zag way. Pellets were broken into pieces to avoid external cracks and used for density measurements. But if there are small cracks which cannot be seen by naked eye, there will be error in bulk density measurements. And also if there is any oxidation, it will be difficult to explain the variation of bulk densities. If porosity is more, magnetic properties will be poorer. But the bulk densities are sufficiently high and these values are not the reason for poor magnetic properties. Because of these reasons, it is difficult to conclude optimum time and temperature for getting higher density.

IV.4.2. Microstructure

Sintered pellets were polished and etched with 2% Nital. But it did not reveal any microstructure. Increasing etchant concentration also did not help. Special etching agents and procedures suggested by Khan et al[39] were used, but were of no use. The same techniques revealed the microstructure of a sintered Sm-Co Japanese magnet. And also, for as-cast samples if base material and additive, these etching agents readily showed microstructure.

X-ray diffraction study of the sintered pellets did not show the peaks correspond to any standard pattern of 2:7, 5:19 and 1:5 phases. There is a deviation in the chemical composition of the sintered pellets (determined by chemical analysis) towards lower RE and Co and higher Fe and lower (RE + Co + Fe). This is observed in the starting powders itself. Annealing of the sintered pellets at 700°C, 800°C and 900°C upto 24 hours and subsequent quenching in water did not improve the magnetic properties.

From the above analysis, it is likely that there is partial oxidation during the process of making these magnets. And also suitable post-annealing treatment may be necessary to be developed for improving the properties. Analysis of the sintered samples for oxygen is necessary.

V. CONCLUSIONS AND SUGGESTIONS

The following conclusions can be drawn from the present work:

1. Optimum parameters determined by taking specific surface area per unit time as a measure of effectiveness of ball milling process are not optimum when $_iH_c$ is a measure of effectiveness of the process.
2. If optimum parameters are determined and maintained, rod milling will have an edge over ball milling, due to narrower particle size distribution.
3. There is a decrease in RE and Co contents and increase in Fe content and decrease in total (RE + Co + Fe) during milling and this deviation increased with milling time. This may be due to partial oxidation of the powders and complex compounds that are forming during dissolution of these powders in concentrated HNO_3.
4. Orientation of the powders is easier when they are mixed with plastic fluid and alligned in a steady magnetic field than when they are field pressed.
5. Pulse magnetic field of 100-200 milliseconds duration is not effective in orienting the powders during field pressing.
6. Very low magnetic properties of sintered pellets may be due to improper annealing treatment and partial oxidation during the processing of these magnets.

It seems worthwhile to carry out the following studies in the light of the conclusions drawn above.

1. Optimum parameters are to be determined for ball milling and rod milling, taking $_iH_c$ as a measure of effectiveness of the process. Experiments to get information about the damage to powders are worth carrying.
2. Residue or complex chemical compound that is formed during dissolution of the powders in concentrated HNO_3 is to be analysed by using PIXE method and X-ray diffraction studies.
3. Field pressing method is to be modified.
4. Sintered pellets are to be analysed for oxygen.
5. Annealing, treatment should be studied thoroughly by varying annealing temperature and time.

REFERENCES

1. Benz M.G. and Martin, D.L. J. Appl. Phys. 43 (1972) 3165.
2. K. Strant, G. Hoffer, J. Olson, W. Ostertag and J.J. Becker, J. Appl. Phys. 38 (1967) 1061.
3. Mc Curie R.A., Carswell G.F. and O'Neill J.B. J. Mat.Sci. 6, (1970) 164.
4. Wernick J.H. and Geller S., Acta Cryst. 12, (1959) 662.
5. Strnat K.J., IEEE Trans. Mag. MAG-6, (1970) 182.
6. Buschow K.H.J., Luiten W., Naastepad P.A. and Westendorp F.F., Philips Tech. Rev. 29 (1968) 336.
7. Buschow K.H.J., Naastepad P.A. and Westendorp F.F., J. Appl. Phys. 40, (1969) 4029.
8. Umebayashi H. and Fujimura Y., Jap. J. Appl. Phys. 10, (1971) 1585.
9. Das D.K., IEEE Trans. Mag. MAG-5, (1969) 214.
10. Cech R.E., J. Appl. Phys. 41 (1970) 5247.
11. Benz M.G. and Martin D.L., AIP Conf. Proc. 5 (1972) 1082.
12. Nagel H. and Menth A., AIP Conf. Proc. 24 (1974) 695.
13. Ratnam D.V. and Wells M.G.H. AIP Conf. Proc. 18 (1974)1154.
14. Benz M.G. and Martin D.L., Appl. Phys. Lett. 17, (1970) 176.
15. Shibata T. and Katayama T., Jap. J. Appl. Phys. 12 (1973) 1020.
16. Jhonson R.E. and Fellows C.J. Cobalt 53 (1971) 191

17. Tsui B. and Strnat K., Appl. Phys. Lett. 18 (1971) 107.

18. Tsui B.Y. and Strnat K., IEEE Trans. Mag. MAG-7 (1971) 427.

19. Martin D.L. and Benz M.G., General Electric Technical Information Series No. 70-C-261 (1970).

20. Charles R.J., Martin D.L., Valentine L. and Cech R.E., General Electric Tech. Inf. Series 71-C-281(1971).

21. Benz M.G. and Martin D.L., J. Appl. Phys. 42 (1971) 2786.

22. Mc Caig M., IEEE Trans. Mag. MAG-6, (1970) 198.

23. Fellows C.J. and Jhonson R.E. Cobalt 56 (1972) 141.

24. Foner S., Mc Niff Jr. E.J., Martin D.L. and Benz M.G. Appl. Phys. Lett. 20 (1972) 447.

25. Gessinger G.H., Lamotte E.De and Buchmann K., IEEE Trans. Mag. MAG-8 (1972) 557.

26. Ojima T., Jomizawo, Yonayama T. and Hori T., IEEE Trans. Mag. MAG-13, (1977) 1317.

27. Jones F.G., Doser M. and Nezu T., IEEE Trans. Mag. MAG-13 (1977) 1320.

28. Soong Hou-ting, IEEE Trans. Mag MAG-14 (1978).

29. Personal communication from Mrs. Padmavathi Sankar.

30. Shankara Prasad K., M.Tech. Thesis, I.I.T. Kanpur (1976).

31. Subramanyam J., M.Tech. Thesis, I.I.T. Kanpur (1978).

32. Rose H.E. and Sullivan R.M.E., A Treatise on Internal Mechanics of ball, tube and rod mills, Orient Longmans Pvt. Ltd. London (1958) Chapter 5.

33. Gaudin A.M., 'Principles of Mineral Dressing' McGraw-Hill Book Company Inc. New York (1939) Chapter 5.

34. Strnat K.J., Olson J.C., and Hoffer G.I., J. Appl. Phys. 39(1968) 1263.

35. Strnat K.J., Hoffer G.I., Olson J.C., and Kubach R.W., IEEE Trans. on Mag. MAG-4, (1968) 255.

36. Narita K. and Yamamato H., IEEE Trans. mag. MAG-14 (1978) 785.

37. Velu E.M.T., M.Tech. Thesis, I.I.T. Kanpur (1977).

38. Personal communication from Mr. E.M.T. Velu.

39. Khan Y. and Zeldmann Jl. of Its Loss-Common metals. 31 (1973) 211